HECTOR (HEC) DESIGN STUDY

SCIENCE CASE DOCUMENT

Rev. No.	Author	Approved for Issue	
		Signature	Date
1.0	Julia Bryant		2016.01.19
1.0	Joss Bland-Hawthorn		2016.01.19
1.0	Warrick Couch		2016.01.19 12:15:48 +11'00'
1.0	Scott Croom		Digitally signed by Scott Croom DN: cn=Scott Croom, o=University of Sydney, ou=School of Physics, email=scott.croom@sydney.edu.au, c=AU Date: 2016.01.21 08:58:19 +11'00'

LIST OF FIGURES AND TABLES

ACRONYMS

R_E	Effective radius
psf	Point spread function
OD	Outer diameter
h_3, h_4	Gauss-Hermite Polynomials, h_3 (skewness) and h_4 (kurtosis) (Gerhard 1993; Van der Marel & Franx 1993)

REFERENCE DOCUMENTS

JvdS_hector_h3_h4_science.pdf	"The assembly histories of galaxies from higher-order kinematic features with Hector" – science contribution paper by Jesse van de Sande & Joss Bland-Hawthorn.
McElroy_hector_report.pdf	"The effects of resolution on IFU studies of AGN physics"
http://www.aao.gov.au/conference/hector-science-workshop	Talks presented at the Hector Science workshop at the AAO, April, 2015.
LukeBarnesHectorReport_final.pdf	"Hector Simulation Report" by Luke Barnes
Will_Hector_RN2.pptx	Will Saunders calculations on read noise.
Fitting_kinematics_using_SAMI_examples.pdf	Note on the galaxy dispersions required based on kinematic fitting of SAMI data.

1 EXECUTIVE SUMMARY

This document presents the science requirements for the Hector instrument based on the design reference mission and feedback from the user community on their science needs. Section 1 discusses the design reference mission, section 2 details the individual science cases, section 3 covers the requirements to meet those science cases, while section 5 then links those requirements to the instrument parameters.

Deciphering the galaxy genome – evolution to individuality

J. Bryant, J. Bland-Hawthorn, S. Croom

Summary

Galaxy evolution is the grandest of all environmental sciences. Just how a galaxy forms and evolves in a given environment is one of the great unanswered questions in astrophysics. Hector is a revolutionary new AAT facility that will obtain integral field spectroscopy for 100,000 galaxies at z ~ 0.1 over ~3000 square degrees. While Hector builds on the success of SAMI, it will enable fundamentally new science that cannot be undertaken with existing or planned instruments. Compared to SAMI, Hector will have a wider field of view (3 degrees vs. 1 degree), higher spectroscopic resolution (R=3000-5500 vs. R=1700-4500) and many more IFUs (100 vs. 13).

The overarching science goal is to understand the physical basis for the diversity of galaxy properties in the local Universe. Substantial steps forward have been possible with smaller surveys such as SAMI, which have sufficient sample sizes to study the properties of galaxies as a function of their mass and local environment, but the diversity of galaxies is driven by more than just these two parameters. The accretion and/or merger history of a galaxy is fundamental to its morphology and star formation history, but to date it has been hard or impossible to capture the diversity of accretion histories observationally. The broader large-scale environment is also known to be important in determining a galaxy's structure via tidal torques. Only with Hector targeting 100,000 galaxies can we hope to probe the detailed physics of galaxy formation in these two extra dimensions of accretion history and large-scale environment.

Specifically, the integral field data from Hector can provide specific angular momentum, higher order velocity moments, mis-alignments between gas and stars as well as measure dynamical disturbance. All of these tracers provide a view into accretion and merger history, which when combined with the unprecedented sample size of Hector will allow us to connect a galaxy's specific history to its current state. By connecting these properties to the network of large-scale structure we will be able to show how accretion is modulated within the cosmic web.

With Hector we will decipher the diversity of galaxies through understanding their individuality.

Introduction

Galaxies share important properties like halos, disks and bulges. But when we look in detail, no two galaxies are identical, and we can see substantial differences even between relatively featureless spheroidal galaxies. Many have tried to identify a surrogate or a twin for the Milky Way. For example, Efremov (2011) identified the 8 best candidates for surrogates, all of which look visibly different. Some of these differences may reflect internal processes and different

stages of evolution, but others may reflect variations in the environment. Interestingly, even the relatively low resolution of the best cosmological simulations today finds that essentially *all* galaxies are different (Naab et al 2014).

The central questions are, ***what are the main drivers of galaxy diversity? And, how do they manifestly influence galaxy properties?*** Galaxy stellar mass widely seen to be the primary driver, with strong trends of mass with star formation (e.g. Peng et al. 2010, 2012), metallicity (Tremonti et al. 2004), and morphology now well characterized. Beyond stellar mass, the next well recognized driver of galaxy diversity is environment. While there has been much debate concerning the best metric to characterize environment, it is now thought that the mass of the host dark matter halo is the primary environmental driver of galaxy properties. It should be noted, however, that the measuring the mass of dark matter halos remains a challenge, particularly at low mass.

Even once stellar mass and dark matter halo mass is accounted for, there remains a huge diversity of galaxy structural properties and star formation histories. It is clear that more than just mass and small-scale environment are required to properly understand the pathways to galaxy growth. The well-established picture of hierarchical growth of galaxies tells us that the accretion history of a galaxy is fundamental to its evolution. For example, does a galaxy go through one or more major mergers, how many minor mergers occur and how much external gas is accreted? Unaccounted for, the stochastic nature of a galaxy's accretion history provides substantial variance in the population, obscuring the underlying physics.

It is also clear that the host halo mass cannot be the only environmental factor. Differences are already seen from small-scale environments between galaxies that are centrals or satellites in a halo. Outside the halo, the large-scale environment defined by the geometry and topology of structure, e.g. within walls, filaments or voids can also modulate the growth of galaxies via both tidal torques and gas accretion.

In summary, the dominant drivers of properties of galaxies are likely to be:

1. Galaxy stellar mass.
2. Host dark matter halo mass.
3. Accretion history.
4. Halo location (central vs. satellite).
5. Large-scale topological environment (walls, filaments, voids etc).

Next generation galaxy surveys need to have sufficient statistical precision to be able to meaningfully span the above parameter space, but more importantly, new breakthroughs will be possible if we have measureables that will enable us to unravel the accretion history of a galaxy. Crucially, integral field spectroscopy gives multiple windows into these important parameters, especially when combined with the latest generations of numerical galaxy simulations (e.g. Naab et al. 2014). Hector will allow us to measure i) specific stellar angular momentum that traces differing merger histories; ii) the higher-order kinematics of the line-of-sight velocity distribution that can differentiate between a variety of formation paths; iii) measure current kinematic disturbance as a probe of ongoing dynamical interactions; iv) measure the mis-alignment between gas and stellar kinematics to identify gas of external origin; v) measure gas phase metallicity gradients as a tracer of external (low metallicity) gas.

On scales larger than a single halo, the global environment defined by large-scale topological structure (filaments, sheets, voids etc.) adds yet another level of complexity. The inflow of gas that fuels star formation is in competition with feedback processes and this inflow of gas is crucially dependent on the *details* of where the galaxy sits within the large-scale structure. Cold flows from filaments deliver the fuel for star formation, but the resulting star formation rate is in turn dependent on the angular momentum from the filament (Benson & Bower 2011). This in turn depends on the alignment of galaxy spins with large-scale structure that simulations predict can be either aligned with filaments (Trowland, Lewis & Bland-Hawthorn 2013) or at the highest halo masses remain perpendicular to the filament (Libeskind et al. 2013). Observational results have shown vastly differing conclusions (Tempel & Libeskind 2013; Tempel et al. 2013; Zhang et al. 2015). The requirement to make a breakthrough in this area is a large-scale survey of galaxies which can measure angular momentum and is carried out in a region which has sufficiently high sampling to provide well defined large-scale structure. Theoretical work by Trowland et al. (2013) and Dubois et al. (2014) suggest 60,000 and 150,000 galaxies respectively are required to disentangle spins with large-scale structure.

The driving parameters of galaxy formation lead to observable differences in a range of dependent quantities that Hector will be uniquely positioned to measure. These include current star formation and star formation history, stellar metallicity and age gradients, gas phase metallicity, angular momentum, kinematic morphology and many others. Bringing all of these together is crucial to uncovering the true nature of galaxies. A prime example is shown in Figure 1. This example from the SAMI Galaxy Survey (Schaefer et al. in prep) is a galaxy in a high-density group environment that has centrally concentrated current star formation (as traced by Hα). This would appear to be an excellent candidate for outside-in quenching (for example from ram-pressure stripping), but the stellar populations of the outer disk are at least several Gyr old and not recently quenched. More telling yet is the kinematics that shows gross misalignment between gas and stellar motions, and stellar metallicity that is lower in the central young stars, associated with current star formation. Bring all this information together we find that this galaxy shows evidence for nuclear triggering of star formation due to external gas accretion, a completely different picture to simple outside-in quenching.

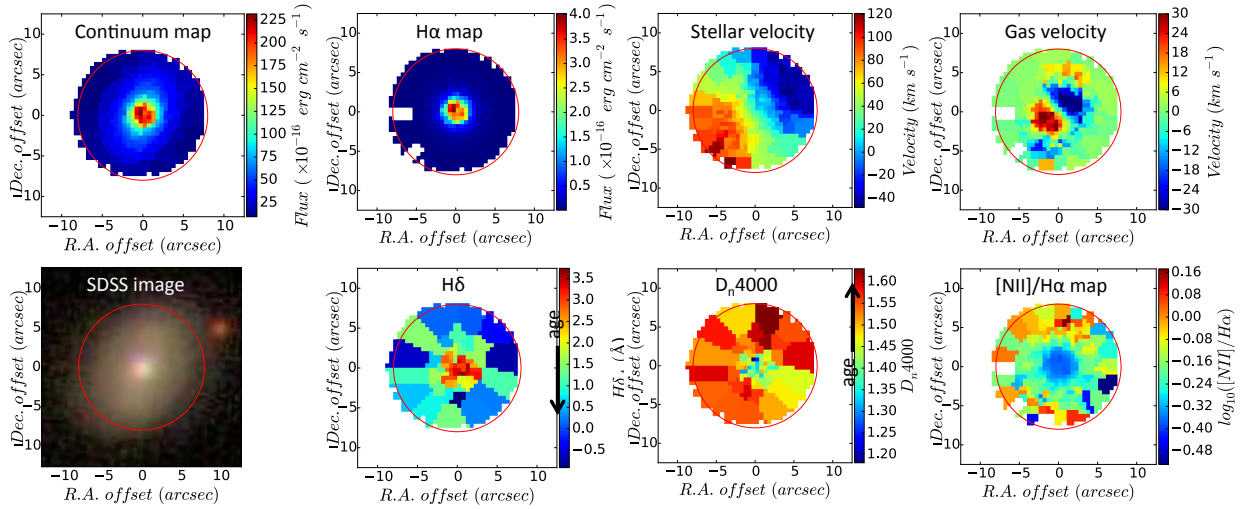

Figure 1:GAMA ID 517302, a highly unique galaxy. SAMI continuum and Hα images (top left & centre left), SAMI stellar and gas velocity (top centre right & right). The star formation is condensed in the galaxy centre compared to the extent of the continuum, and

the gas and stellar velocities are highly misaligned. SDSS image (lower left), Lower centre left and right show the radial distribution of effective ages measured by emission-subtracted Hδ absorption equivalent width index and the D_n4000, showing that the stars at higher radius are older. [NII]/Hα ratio map (lower right) shows elevated [NII]/Hα toward the edge of the galaxy which may indicate shocks or a post-AGB stellar population. Images from Adam Schaefer.

The Hector observations need to be paired up with detailed analysis of the local and extended environment of each galaxy, and this can be provided by next generation galaxy surveys such as TAIPAN and WAVES. Coupled with this, the surveys for HI gas using ASKAP supply the missing neutral gas that cannot be detected in the optical. Hector, ASKAP and TAIPAN/WAVES then provide a fantastic synergy that will allow us to delve into the details of a galaxy's formation history like never before.

Hector will be the first spatially-resolved IFU survey with the >60,000 galaxies, necessary to span the parameter space described above and connect its physical characteristics to its stellar mass, small-scale environment, large-scale environment and accretion history. Specifically, Hector will do this by:

1. Correlating the signature of fast and slow rotators with the new detailed environment measures to investigate the influence of the angular momentum of material feeding into galaxies on the individuality of galaxies within different large-scale structures (see Sections 2.1.1 to 2.1.3)
2. Directly measuring the higher-order kinematics signatures to trace the individual galaxy formation histories and how these lead to different current structural properties, and are modulated by environment (see Section 2.1.1).
3. Using measurements of non-regular kinematics to identify dynamical disturbance in galaxies as tracers of merger history (see Section 2.3.4).
4. Measuring stellar-gas kinematic misalignment directly to trace the impact of mergers on the star formation and identify the origin of gas and stars in galaxies (see Section 2.1.4 and 2.3.7).
5. Spatially resolving star formation rates, stellar ages and metallicities to trace the build up of mass and how that evolution was influenced by accretion history and the detailed environment (see Sections 2.3.3 and 2.3.6).
6. Measuring stellar populations from absorption lines in order to trace the star formation histories (see Section 2.2).
7. Directly identifying outflows from kinematic signatures and emission line diagnostics of shocks and AGN, and evaluating the balance of gas supply for star formation in all environments (see Section 2.3.1 and 2.3.2).

These new "measurables" will decode each galaxy's genome that defines its individuality and will then unpick the strongest impacts on the history of that galaxy's formation. The new innovation offered by Hector is the combination of a huge galaxy sample with the rich diversity of information enabled by high-resolution integral field spectroscopy. These are both necessary (as shown above) to understand the complex interaction of mass, environment and accretion history on angular momentum, structure formation and stellar mass growth. Never has there been a large enough observational sample to apply these techniques and then directly compare to the simulations. Hector will be the only instrument capable of reaching the galaxy numbers required in the near future because of the survey efficiency afforded by the unique combination of the 3

degree field and a telescope on which major surveys are valued, such that a very large program is possible.

2 SCIENCE CASES

A Hector Science Workshop was held in April 2015 as a community forum to present science cases from the community for use with Hector. Input from the community was sought as talks, written science contributions and reports, and the summary of those cases is presented in sections 2.1-2.4. These cases expanding on the detailed investigations required to fulfil the key Hector science presented in Section 1. In an effort to give a complete representation of the community views, all science cases presented have been included even where there is some overlap. When text was not supplied by the community member, the science case was written by J. Bryant based on presented talks and discussions.

The science proposals below are grouped by similar instrument requirements. Many science cases will be met by the requirements discussed more generally as stellar kinematics, stellar populations, and gas physics (kinematics, abundances and diagnostics). The aim here is to cover enough of these (as presented by the community) to fully define the instrument requirements.

2.1 Stellar kinematics

The merger history of galaxies is encoded in the stellar kinematics. As such, there are many science cases that are based on accurate stellar rotation and dispersion measures. All are dependent on the precision with which these can be measured. The main science cases are broadly outlined then the requirements are listed at the end of this section.

2.1.1 Assembly history of galaxies from higher-order kinematic features

(Including some input from report "JvdS_hector_h3_h4_science.pdf" by Jesse van de Sande & Joss Bland-Hawthorn)

For fast rotating galaxies a strong anti-correlation exists between the higher-order Gauss-Hermite moment h_3 and the anisotropy parameter v/σ. Recent cosmological hydrodynamical simulations suggest that with new integral field spectrographs such as Hector, it is possible to connect the observable higher-order stellar kinematic features in galaxies to their cosmological assembly history. These simulations show that fast rotators with gas-rich merger histories have a strong h_3-(v/σ) correlation, while fast rotators with gas-poor mergers do not, due to the absence of a dissipative gas component. Accurate measurements of stellar line profiles therefore provide strong constraints on models of galaxy formation, as deviations from a Gaussian line profile indicate anisotropic orbits of stars or rotating stellar bodies within elliptical galaxies. Hector's ability to accurate measure the shape of the absorption-line profiles will therefore provide us with detailed knowledge and new insights in the kinematic structure and assembly histories of galaxies.

This study requires that the Hector galaxy sample can be divided into several fundamental properties that determine a galaxy's evolution, namely stellar mass, morphology, and environment. We propose to study 6 stellar mass bins between 10^9 - $10^{12} M_*/M_\odot$, three different morphological types (Elliptical, S0, and (Barred)-Spirals), for galaxies in the field, in groups,

and in clusters. From Naab et al. (2014), the ATLAS3D survey, and preliminary results from SAMI, we furthermore know that we can expect at least four different classifications when using the higher-order stellar kinematic features. One class has a strong anti-correlation between h_3 and v/σ, likely due to the presence of a dissipative gas component during the merger, while the second class has no such correlation, and likely had dry-mergers in its past. The third class consists of galaxies with a strong bar, which reveals itself in a more peanut shaped h_3 versus v/σ and h_4 correlations with v. The fourth class are the counter rotating cores in slow rotators, where a strong h_3 and h_4 is clearly present in the two-dimensional maps.

The need for a large range in stellar mass makes this a unique project that can only be done by Hector with a spectral resolution of 1.3Å. This is because the lower spectral resolution in the blue found in SAMI and MANGA, significantly reduces the fraction of galaxies for which h_3 and h_4 can be measured in the lower stellar mass bins (see detailed discussion in Section 2.1.6 below). Based on the lower spectral resolution of the next largest survey, MANGA, and Figure 3 below, MANGA will struggle to get h_3/h_4 measurements on galaxies with sigma<~200km/s, which limits them to galaxies with stellar masses of $>10^{10}$ or even $10^{10.5}$ $M_*/M_\odot$. With 1.3Å resolution, however, in the lowest stellar mass bin of $<10^{9.0}$ $M_*/M_\odot$, a 100,000-galaxy Hector survey will have up to 15,000 galaxies (see the Hector galaxy survey simulation, Section 4.4.3). Of those galaxies, there will be a ~1/10 detection rate of h_3/h_4 based on estimates from dispersion distributions of SAMI galaxies and the requirement of sigma>50km/s, which will leave 1500 galaxies in that mass bin. In order to have statistically useful bins with 30 galaxies per bin, 3 morphological types and 3 environments for 4 different kinematic classifications, requires 30x3x3x4 =1080 galaxies in each of 6 stellar mass bins. Therefore, since a very large sample is required in order to get ~1000 low stellar mass galaxies with h_3/h_4 measurements, this science is therefore *uniquely* possible with Hector with 1.3Å spectral resolution (sets the dispersion limit) and 100,000 galaxy survey size - the fraction of galaxies with measurable h_3/h_4 is too low for any other survey.

2.1.2 Impact of environment and morphology on the formation of fast and slow rotators

(Including some input from Lisa Fogarty)

The stellar kinematics of galaxies provide a unique insight into the different dynamical processes driving galaxy formation. For instance, early-type galaxies are found to fall into two major kinematic groups, fast rotators and slow rotators (Emsellem et al. 2007), when classified according to their angular momentum. Slow rotators turn out to be some of the most massive galaxies in the Universe, so understanding their origins places constraints on hierarchical galaxy formation.

Slow rotators are often found in the cores of dense galaxy clusters and may be formed there by dynamical processes dominant in clusters. However, recent work using the SAMI Pilot Survey and SAMI Galaxy Survey have found evidence that slow rotators can also form in group environments (Fogarty et al. 2014). In addition recent simulations have shown that slow rotators can form through a variety of evolutionary paths, involving major and minor merging to different degrees (Naab et al. 2014).

To fully understand the evolution of slow rotators it is necessary to study the kinematics of galaxies across a wide range of environments and stellar mass. Large-scale integral field spectroscopic surveys enable these measurements and progress our understanding of the dynamical processes of galaxy evolution.

2.1.3 Angular momentum in galaxies

Dynamical processes such as tidal interactions create morphological transformations (Bekki & Couch 2011). The study of galaxy angular momentum and morphology in SAMI field, group and cluster galaxies has shown the power of IFU spectroscopy in this field (Fogarty et al. 2015; Cortese et al. 2015). However, the larger galaxy sample afforded by Hector will not only increase the significance of these results with more galaxies in a range of environments including a larger variation in clusters, but in addition, if Hector can extend the redshift range further than SAMI to z>0.1 then direct comparisons can be made to evolutionary tracks from modelling.

To understand morphological transformations in galaxies relies on IFU observations to larger effective radii. Two examples are firstly, that the outer parts of galaxies are particularly important in distinguishing between ram pressure stripping and starvation mechanisms for quenching of star formation, and secondly, angular momentum requires galaxies to be imaged to larger radii than is currently achieved with SAMI. How large is dependent on the stellar mass and specific angular momentum profiles. Romanowsky & Fall (2012) studied the relationship between stellar specific angular momentum and stellar mass of galaxies out to $10R_e$ in a small sample of galaxies and found that data out to $2R_e$ are sufficient to give reliable estimates of specific angular momentum. Figure 2 is taken from Romanowsky & Fall (2012) and shows that $1R_e$ only captures 50% of the specific angular momentum in disk galaxies but $2R_e$ encloses ~75%. In spheroidal galaxies, ~30% of the specific angular momentum is within $2R_e$, but an unrealistically high radius is required to include >50% of the specific angular momentum in spheroids. *Hector can therefore measure reliable specific angular momentum for most galaxies based on the Romanowsky & Fall (2012) results, if most galaxies are imaged to 2Re.*

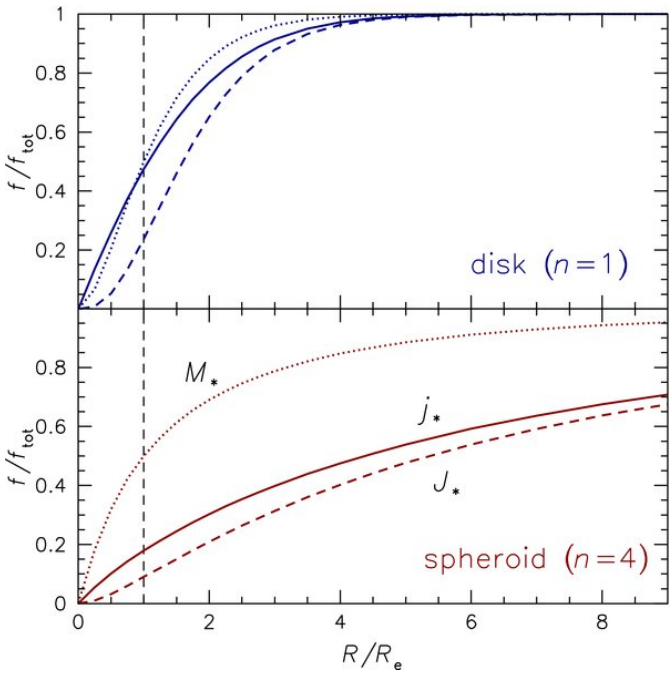

Figure 2: Cumulative fraction of enclosed mass and angular momentum vs radius normalised to Re, for model galaxies from Romanowsky & Fall (2012). Top: galaxies with an exponential (n=1, disk) profile. Bottom: galaxies with a de Vaucouleurs (n=4, spheroid) profile. Three quantities shown are projected stellar mass (dotted lines), angular momentum (J; dashed lines) and specific angular momentum (j*; solid).*

2.1.4 Misalignments and the origin of gas in galaxies

This science case is discussed below in the gas kinematics section 2.3.7. It combines both gas and stellar kinematics, and therefore relies on the measurement of the position angle of stellar rotation. These fits require a continuum S/N>5/Å in >5 spatial elements across a galaxy. Large samples across different environments and stellar masses are essential to investigate how the environment impacts the accretion of gas into galaxies.

2.1.5 Scaling relations

Cortese et al. 2015 showed how all galaxies in v0.8 SAMI data could be unified on a Universal dynamical scaling relation (between stellar mass and velocity quantified by $S_{0.5}$) irrespective of morphology. This relation highlights the link between the kinematics and baryon content of a galaxy and is a less biased comparison to theoretical models because it does not require any pre-selection in the sample. A substantial galaxy sample from Hector would allow the Cortese analysis to be extended to investigate hints of a break in the relation at lower stellar masses, as well as confirm the consistency of the relation across morphological types.

The Fundamental plane links the stellar velocity dispersion to the effective radius and mean effective surface brightness. Understanding the impact of galaxy properties, morphologies, and environments requires fitting the form of the Fundamental plane for sub-classes of objects. This can effectively be done with a massive Hector-type sample that will allow galaxies types to be subdivided, while maintaining the statistics to fit the plane and compare the difference in outliers. The ability to measure sigma out to larger radii (at least $2R_e$) is important to give a more

accurate velocity dispersion measure and a tighter fit to the Fundamental Plane than has been achieved any previous large galaxy surveys.

2.1.6 Requirements for spectroscopic measurements (stellar kinematics)

Sections 2.1.1- 2.1.5 discussed science that primarily relies on fitting of the continuum to extract stellar kinematics. In this section we discuss the requirements in order to measure stellar velocities, dispersions and higher order moments required for that science. Detailed simulations for Hector by Jesse van de Sande have assessed the required S/N, resolution and wavelength range for dispersion, h_3 and h_4 measures. The full report is available, and excerpts from the report are discussed here. We focus the requirements on the constraint for measuring h_3 and h_4 because they are generally tighter than measuring dispersion alone.

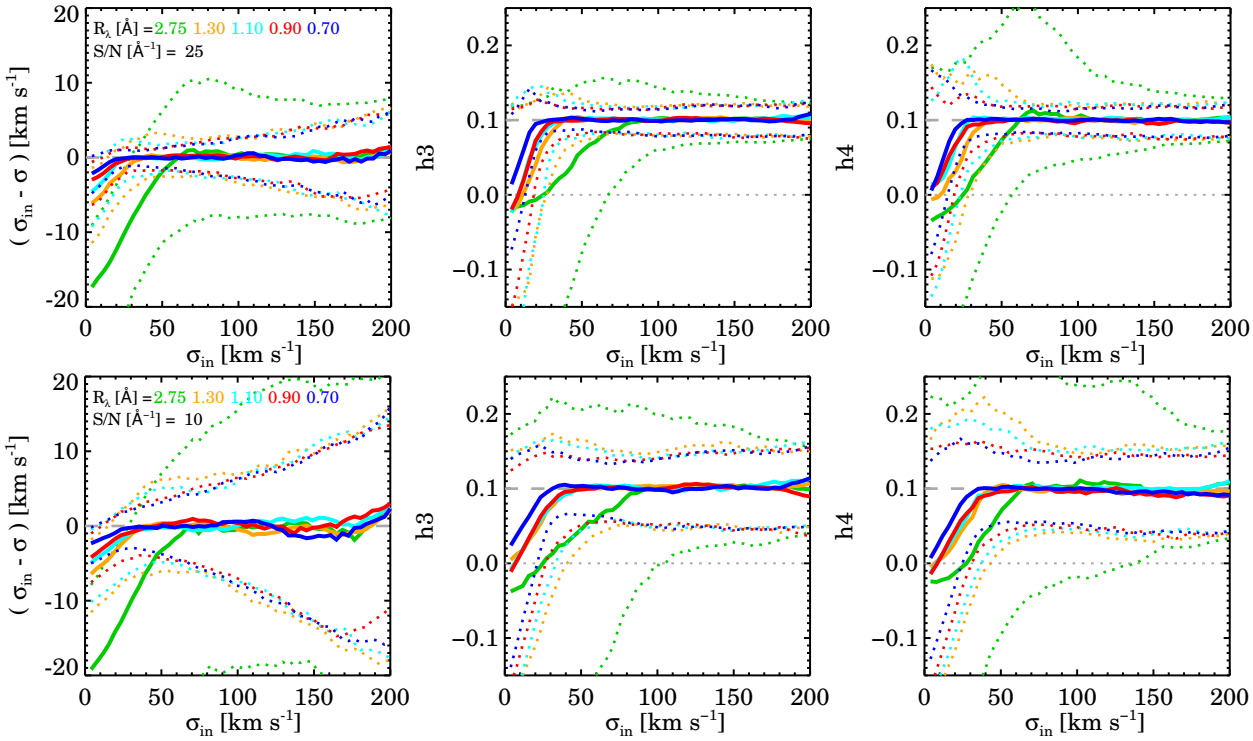

Figure 3: Impact of the resolution on the recovered kinematics. From top to bottom S/N = 25 and 10/Å. Different colours show different resolutions with R=2.75 matching the blue resolution of SAMI. In the left column, the lines show the 50th (median, solid line), 16th and 84th percentiles (1σ errors, dotted lines) of the differences between the measured values and the input values of the velocity dispersion σ_{in}. The middle and right column show the recovered values of h_3 and h_4, compared to the input values of 0.1 (dashed line). Reproduced from Fig. 9 of Van de Sande's report. In order to measure h_3 and h_4, the dotted lines need to be <~0.1 apart (lower dotted line must stay above 0.0). Therefore in the S/N=10/Å case (bottom row), a resolution of 1.3Å or better is required

to measure stellar kinematics in galaxies that have σ_{in}>40km/s, whereas the resolution of SAMI (R~2.75) limits the galaxies in which h_3 and h_4 can be measured to having σ_{in}>~130km/s.

Figure 3 shows that higher spectral resolution and higher S/N allow σ, h_3 and h_4 to be measured in galaxies with lower effective velocity dispersion (σ_{in}). Figure 5 shows the distribution of σ_{in} for the SAMI galaxies (which have a similar sample selection to the potential Hector galaxy survey; see section 4.4.3). 50% of the galaxies have dispersions <75km/s, and they are predominantly in the lower stellar mass regions with masses $<10^{9.5}$ $M_\odot$. Lower stellar mass galaxies also have lower S/N as illustrated in Figure 6 from SAMI in Allen et al. 2015. The Hector S/N will be similar to that of SAMI as the hexabundle and fibre cables will have similar throughputs, but the spectrograph should have improved transmission. It is clear that since the stellar kinematics are critical across several stellar mass bins, the requirements must be set based on a S/N~10/Å so that the lower stellar mass galaxies have measureable σ, h_3 and h_4 and also in order to measure kinematics to higher radii in higher the mass galaxies.

The ability to measure h_3 and h_4 is dependent on:

1. the dispersion of the galaxy: More massive galaxies tend to have higher dispersion, but fast and slow rotators can occur in all mass ranges. Results from SAMI indicate that in order to measure stellar kinematics for most galaxies, requires measuring galaxy dispersion down to σ>~30km/s (see supporting document "Fitting_kinematics_using_SAMI_examples.pdf").
2. the spectral resolution: required to be high enough to enable measurement of galaxy dispersions down to ~30km/s (ideally 20km/s). This can be measured with an instrumental resolution of ~60km/s (ideally 40km/s) for high S/N. However, in the lower S/N regime found in the outer parts of galaxies or fainter galaxies, the resolution requirements are stricter. Modelling in Figure 3 based on the S/N=10/Å, shows that a spectral resolution of 1.3Å is required in order to measure the stellar kinematics for galaxies that have velocity dispersions (σ) down to 40km/s. Based on the SAMI v0.8 data ~82% of galaxies have σ>40km/s and therefore a cut of 40km/s will only exclude ~18% of the sample. If the resolution is improved further, Figure 3 shows that this dispersion cut-off does not change appreciably. Relaxing the resolution to 2.3Å limits the measurable galaxies to those with dispersions >150km/s, removing most of the sample.
3. the S/N (Table 1 has a summary of the following examples): High S/N~50/Å allows h_3 and h_4 to be measured to σ~20km/s. The limiting useful S/N however is ~10/Å. When stellar kinematic fits are done for spectra with a continuum S/N=10 (see Figure 4) over the wavelength range of 3700-7000Å, the h_3 and h_4 indices can be measured in galaxies with dispersions down to ~40km/s. The particular simulation example in Figure 10 (1.3Å resolution, 4 hour exposure/7 dithers, dark time, 100μm fibres) shows that Hector will achieve S/N=10/Å in the far blue for galaxies with surface brightness at $1R_e$ of r(SDSS AB)<22.0-22.5 mag/arcsec^2 when the outer row of 24 cores is binned. Based on Figure 8 and Figure 10 that is ~60-70% of the blue or magenta simulated galaxy sample depending on galaxy type (Not all will have σ>40km/s). However, for a larger fraction of galaxies, S/N>10/Å is attainable over a reduced wavelength range. Truncating this wavelength range to 4700-7000Å as in Figure 4, will allow h_3 and h_4 measures in galaxies with dispersions down to ~60km/s, and the same S/N simulation above predicts S/N>10/Å in that wavelength range for r<24 mag/arcsec^2, which occurs at $1R_e$ for ~95% of galaxies

when binned by 24 cores. **This is a substantial improvement on what can be achieved by SAMI or MANGA due to the improved resolution of Hector.** In order to measure h_3 and h4 in galaxies with dispersions down to 30km/s requires a S/N>30/Å from 3700-7000Å or SN>40/Å from 4700-7000Å, which will be achievable for surface brightness of r<21 and 22.6 mag/arcsec^2 respectively in 24 binned cores.

4. the wavelength range over which the continuum is fitted. Note that in Table 1, the largest fraction of galaxies observable is when the continuum is fitted over 4700-7000Å, rather than to lower wavelengths. With a S/N=50 and a S/N=10, the same fraction of the population is observable but it is a different population with the latter extending to fainter, lower-mass galaxies.

Table 1: Example of the velocity dispersions of galaxies (σ_{in}) that allow measurement of h_3 and h_4 indices when the continuum is fitted over the wavelength range in column 2, with the required minimum S/N in column 3. The faintest r-band magnitude (based on the Sersic index>1.5 galaxy population) that can then be observed with that S/N is in column 4. The fraction of the galaxy distributions from the Hector Survey Simulation code (see Section 3.1) that meet that surface brightness limit at 1R_e based on the S/N simulation (detailed in Section 3.2) is then multiplied by an estimate of the fraction of galaxies with a velocity dispersion greater than the value in column 1 (based on SAMI DRv0.8) to give the fraction of galaxies that will have stellar kinematics observable.

σ_{in} (km/s)	Wavelength range for continuum fitting (Å)	Min S/N (/Å)	Faintest r limit (mag/arcsec^2) (Sersic>1.5)	Frac. galaxies within r limit at 1R_e * frac. with $\sigma > \sigma_{in}$ = total measureable.
20	3700-7000	50	20.0	0.03*0.96=0.029
20	4700-7000	50	22.4	0.73*0.96=0.70
30	3700-7000	30	20.8	0.15*0.88=0.13
30	4700-7000	40	22.6	0.78*0.88=0.69
40	3700-7000	10	22.0	0.60*0.82=0.49
60	4700-7000	10	24.2	0.96*0.67=0.64

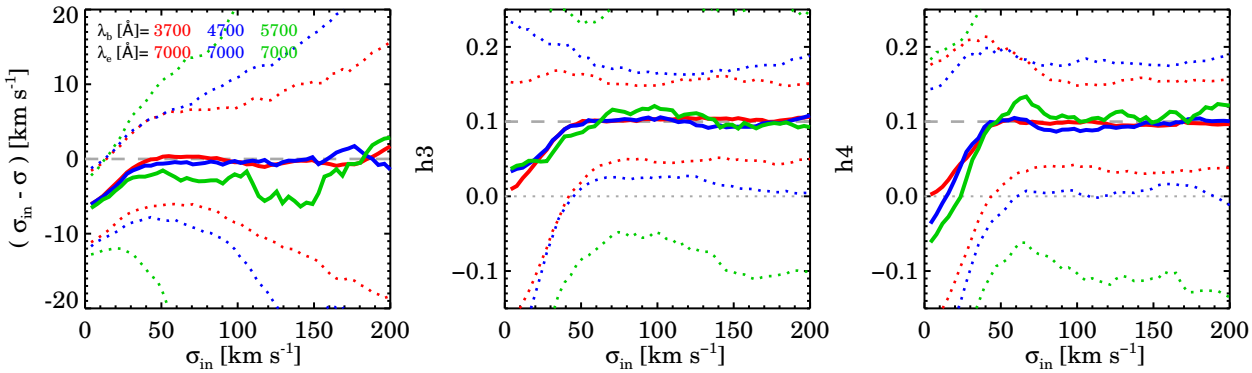

Figure 4: Effect of changing the minimum wavelength over which the continuum is fitted for kinematics. Plots are as in Figure 3 except that the colours of the lines denote the wavelength range and the S/N is set to 10/Å. h_3 and h_4 can be measured in galaxies with dispersion of >~40km/s when the continuum is fitted from 3700-7000Å. However, the S/N drops rapidly in the far blue. Therefore, if the S/N>10/Å from 4700-7000Å, then dispersions of > ~60km/s can be measured.

Further results from the van de Sande report (see report for details):

- If the wavelength range starts at ~3700Å, an upper wavelength redder than 5500Å has no improvement in the ability to measure σ, h_3 and h_4.
- Psf shapes for Gaussian, direct imaging and pupil imaging were provided by Will Saunders. The effect of a mismatch in the psf of the template was found to have no impact on the ability to measure stellar kinematics. We note, however, that all 3 psfs were very similar. Note also that a stellar library of ~1000 stars with matching psf could be completed with Hector in only ~5 nights of bad seeing (assuming faster readout than AAOmega).
- If the spectrograph has a fixed dispersion (A/pix), there is (a) little benefit in going to a sampling coarser than 2.0 pix/FWHM, because the benefit of higher resolution is almost entirely counteracted by the penalty from under-sampling; and (b) little penalty in going even to 2.4pix sampling. At lower S/N~10, there is a small advantage in higher resolution with lower sampling, compared to lower resolution with higher sampling.

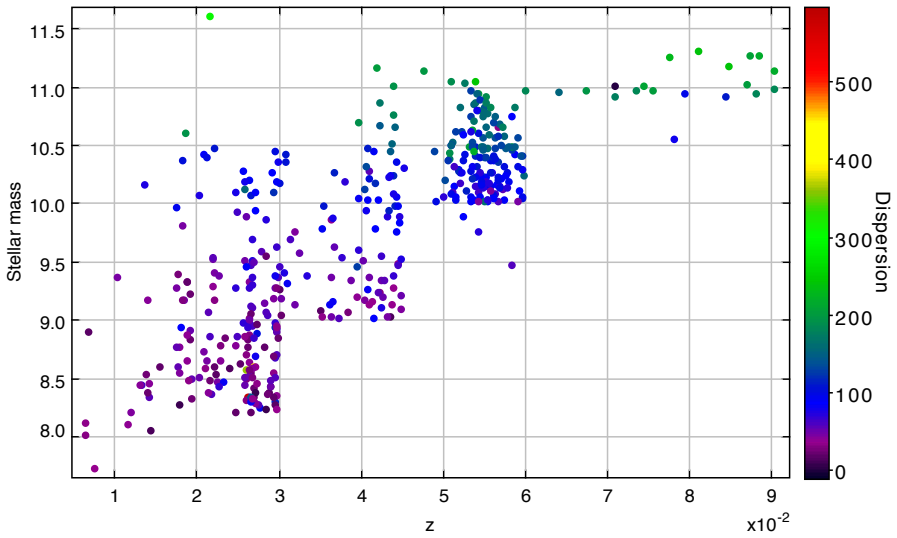

Figure 5: Redshift versus stellar mass versus dispersion (σ) for galaxies in the SAMI survey (v0.8 release). The Hector galaxy survey will have a very similar selection. 50% of the galaxies have dispersions<75% and they lie in the lower stellar mass region. S/N in the lower stellar mass galaxies in SAMI is 10/pix or less in the central arcsec for galaxies with stellar mass <~$10^{9.5}$ $M_{\odot}$.

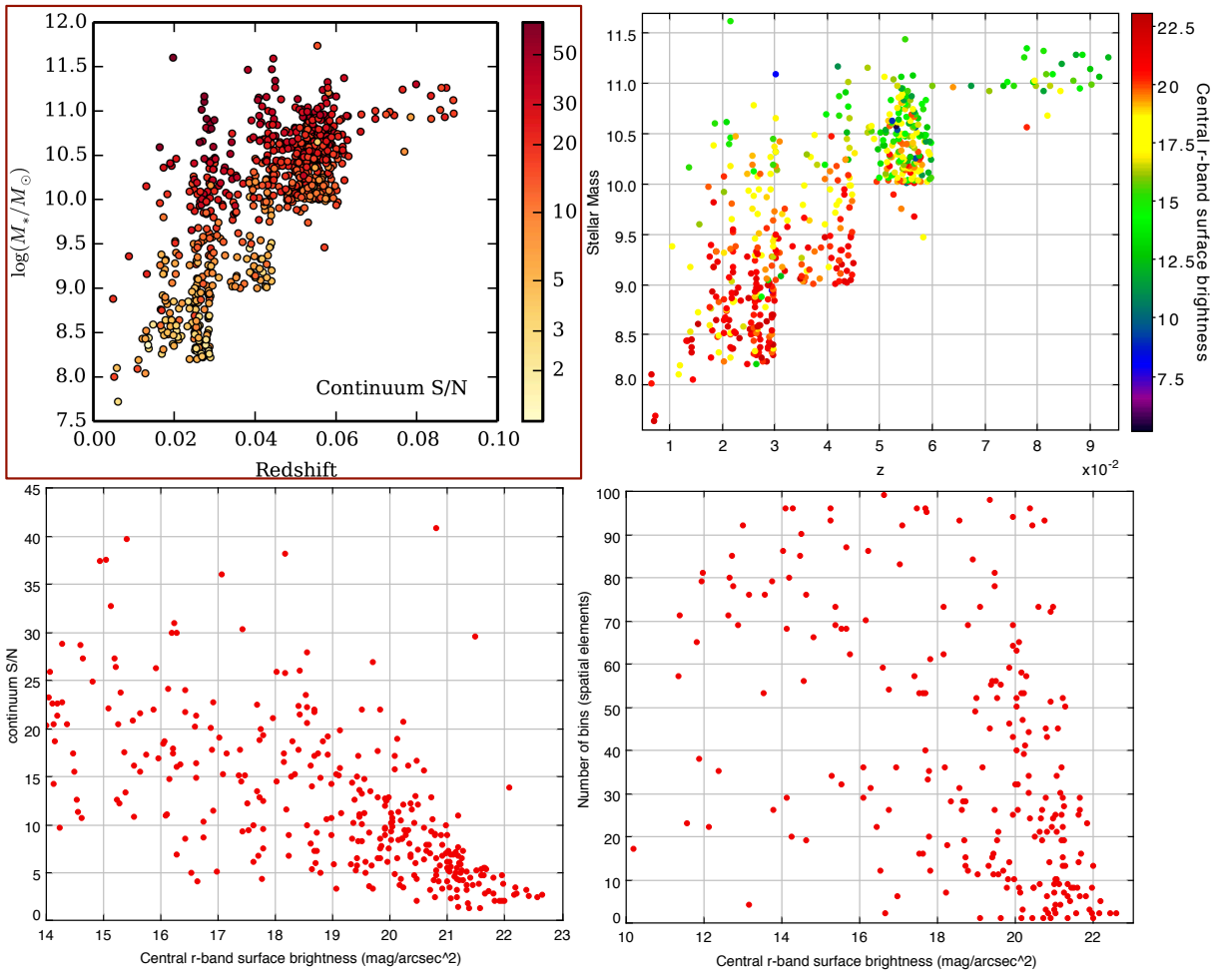

Figure 6: Top left: Redshift versus stellar mass versus continuum S/N per pixel (averaged over the blue arm) within 1 arcsec, for SAMI galaxies from v0.8 (Allen et al. 2015). Most galaxies with stellar masses $<10^{9.5}$ $M_{\odot}$ have a central S/N<10/pix. The Hector S/N will a little better. Top right: Redshift vs stellar mass, colour coded by central r-band surface brightness. Surface brightness of >~20mag/arcsec^2 achieve a S/N<10/pix, while S/N>20/pix is typical for surface brightnesses<~19mag/arcsec^2. Lower: Central r-band surface brightness vs continuum S/N (left) and number of bins to reach S/N=10/pix (right). The plots are truncated in both axes to highlight the faint end. Surface brightnesses fainter than ~21 mag/arcsec^2 require binning to reach S/N=10/pix, and the majority of those have > 5 bins (spatial elements) with S/N>10/pix across the galaxy.

Summary of stellar kinematics requirements:

- Resolution: *Aim*: blue spectral resolution of 1.3Å from ~3727 - 7000Å. *Requirement* 1.3Å from ~3727 - 5700Å (no advantage in any better resolution).
- S/N: *Aim*: continuum S/N ~20 from 4700-7000Å at 1 R_e. *Requirement:* S/N=10 4700-7000Å at 1Re.
- The number of pixels sampling the FWHM has little impact on the σ_e if the resolution is scaled with respect to the sampling. *Requirement*: psf shape must be accurately known for the instrument.
- The effect of a non-Gaussian instrumental psf has no impact on the limiting σ_e , if the template stellar library is convolved with the same instrumental psf.
- Wavelength range: *Aim* $3700 < \lambda[Å] < 7000$. *Requirement:* $3700 < \lambda[Å] < 5500$. Small gaps in the wavelength coverage is OK.
- Bundle size: *Requirement*: spatially resolved out to ~ 1 R_e (minimum), with an *aim* for 2 R_e (for angular momentum in particular).
- Spatial sampling: 4-5 independent spatial elements along a given diameter (minimum) across a galaxy.

2.2 Stellar populations

(Including some input from Nic Scott)

A galaxy's stellar population preserves a record of the entire history of its past evolution. Large, single-aperture, spectroscopic surveys have been incredibly successful in revealing how global stellar ages, metallicities and abundances vary with other key galaxy properties, and in so doing identifying different evolutionary regimes for galaxies. However, their lack of spatially resolved information severely limits their ability to separate competing physical mechanisms. Key

diagnostics like age and metallicity gradients are required to distinguish between inside-out or outside-in formation models - radically different processes that yield similar global average properties. Such measurements are only possible through integral field spectroscopy.

While small-scale IFS surveys are beginning to accurately measure spatially resolved stellar populations they lack the statistical power to disentangle the effects of the many competing parameters at play in galaxy evolution. Mass, morphology and environment are all thought to influence a galaxy's evolutionary history, however their effects are highly degenerate. Only a survey with a large sample of many thousands of galaxies with integral field, moderate S/N spectra can robustly determine how stellar population gradients vary with these three key parameters.

Requirements for stellar populations:

- Wavelength range: *Requirement* is 3850-5500A. *Aim* of coverage of IMF sensitive features (NaI, CaII, FeH) at 820, 860 and 990 nm would also enable IMF science that may not be possible (never been tested) using the blue absorption lines.
- Sky subtraction: Robust subtraction of sky emission lines over this region to a *requirement* of ~ 0.5% accuracy, and an ideal *aim* of 0.1%.
- S/N ~ 20/bin (averaged across the blue arm) in at least 5 spatial bins.
- Resolution *requirement* of 8.4Å FWHM (σ=280km/s at 3850Å) and target of 2.5Å FWHM (σ=84km/s at 3850Å).
- Galaxies with stellar masses $>10^{9.5}$ would be a requirement, but an aim would be to reach to lower stellar masses at z<0.02.

2.3 Emission line science on winds/outflows, ionisation diagnostics and metallicity.

(Based on a discussion paper from Anne Medling, Lisa Kewley, I-Ting Ho, Rob Sharp, Elise Hampton, Rebecca Davies along with talks from the Science Workshop, as well as additional direct contributions from the community.)

This section groups together the requirements for science cases involving emission line fitting, along with details of modelling of those requirements.

Accurate deblending of emission lines into components is crucial for many science cases. Contributions from the community on emission line science are within the following overlapping categories:

1. Detecting winds and outflows in galaxies.
2. Separating star formation and AGN processes and identifying shocks with ionisation mapping.
3. Galaxy metallicities and chemical abundance mapping.

4. Kinemetry.
5. Scaling relations using gas rotations and dispersions.
6. Mapping star formation from H-alpha for comparison with environment, morphology, radio emission.
7. Misalignments and the origin of gas in galaxies.
8. Environmental processing in filaments and the link to HI.

2.3.1 Winds and outflows

(Based on a contribution from Anne Medling)

In the standard picture of galaxy formation and evolution, the mass of galaxies is built up hierarchically through successive mergers. Large-scale gas flows combined with central bursts of star formation are critical for transforming merging galaxies (e.g., Kauffmann et al. 1993, Springel et al. 2005, Hopkins et al. 2008, 2009a,b). During the merger, gas collisions and associated shocks trigger star formation (e.g., Barnes 2004, Chien & Barnes 2010). As the galaxy disks become disrupted by tidal effects, gas flows toward the central regions where nuclear starbursts may be triggered (Barnes & Hernquist 1996; Mihos & Hernquist 1996; Iono et al. 2004; Springel et al. 2005) or supermassive black holes may be fueled (Springel et al. 2005, Hopkins & Hernquist 2006). At very late stages of the merger, starburst- or AGN-driven winds can drive gas back out of the central regions (Narayanan et al. 2008). These winds force massive shock fronts into the surrounding gas (c.f. Crocker et al. 2014), illuminating their path and providing a bright observational signpost for galaxies currently undergoing massive structural rearrangement.

Despite the importance of major gas flows in galaxy formation and evolution, their detailed physics remains poorly understood. Until recently, observational studies were mostly limited to velocity maps of neutral gas in a few nearby galaxies, targeting the most extreme systems. With the increasing popularity of integral field spectrographs, the number of galaxies with wind detections has likewise increased. In particular, large integral field surveys such as the SAMI Galaxy Survey (Croom et al. 2012, Bryant et al. 2015) have the capability to detect winds in *normal* galaxies (Ho et al. 2014). Gas flows are often easily identified from signatures of shock emission produced as the gas moves through the multiphase interstellar medium; these shocks produce elevated velocity dispersions and key emission line ratios (particularly [S II]/Hα and [O I]/Hα; Veilleux & Osterbrock 1987, Allen et al. 1999, Rich et al. 2010, 2011, 2014, Ho et al. 2014).

Galaxies with extreme winds (in which the luminosity from the shock-excited gas outshines the emission from the host galaxy (e.g. from photoionization from stars and/or an AGN) are thus easily detected by optical spectroscopy by comparing emission line ratios and their line widths. However, low-level winds naturally have a smaller effect on the line ratios and widths that are difficult to disentangle from the host galaxy contribution. Hector will bypass this challenge using two key strategies: 1) By spatially resolving the galaxy, Hector will enable kinematic and spectral modelling of the host galaxy (e.g. a star-forming disk). Once this model is subtracted, the residuals can be analyzed for signatures of outflows. 2) With high spectral resolution (R>4500), emission lines in an individual spectrum can be separated into multiple kinematic components (as in Ho et al. 2014). In the case of a wind galaxy, this line decomposition often

results in a narrow peak corresponding to the galactic ISM photoionized by star formation (and thus with star-formation-like line ratios) and a broader (red- or blueshifted) peak corresponding to the gas flow (with shock-like line ratios). By combining this spatial and spectral resolution, Hector will measure the strength and spatial covering fraction of gas flows in galaxies in the local universe. This census of winds, and the accompanying energy and geometry measurements of the gas flows, are key to understanding the fuelling of galaxy evolution.

2.3.2 AGN-SF separation

(Based on text from Rebecca Davies)

The relationship between star formation and AGN activity is one of the most significant unsolved problems in galaxy evolution. Scaling relations between black hole mass and host galaxy properties such as stellar velocity dispersion, bulge mass and bulge luminosity strongly suggest that black holes grow simultaneously with their host galaxies (e.g. Kormendy & Richstone 1995, Magorrian et al. 1998, Gebhardt et al. 2000, Ferrarese & Merritt 2000). AGN activity may regulate star-formation in the host galaxy, or circumnuclear star-formation may play an important role in fuelling the accretion activity of the central supermassive black hole. However, there is little agreement in the literature regarding the impact of AGN activity on star formation. Several studies have found the star-formation rates (SFRs) within AGN host galaxies to be comparable to or greater than the SFRs of inactive galaxies at the same stellar mass and redshift (see e.g. Silverman et al. 2009, Mullaney et al. 2012, Karouzos et al. 2014). These findings are supported by an apparent anti-correlation between stellar age and the fraction of galaxies hosting active nuclei (Silverman et al. 2009). However, there are many examples of galaxies in which star-formation appears to have been quenched or suppressed by powerful galaxy-scale outflows driven by energy released during accretion episodes associated with luminous AGN or QSOs (Croton et al. 2006, Schawinski et al. 2007, Nesvadba et al. 2010, Maiolino et al. 2012). Radio AGN, characterised by very low Eddington ratios, are often hosted by red sequence galaxies.

The lack of clarity in the current picture of AGN-host galaxy co-evolution is likely to be driven primarily by two factors. First of all, it is clear that the impact of AGN activity on star formation is dependent on AGN luminosity and Eddington ratio, and therefore the observed relationship between star-formation and AGN activity is strongly impacted by limited or incomplete samples. Secondly, integrated star formation rates and average ages reflect the average properties of galaxies but provide limited insight into the physical processes governing the interplay between star formation and AGN activity. Suppression of star formation in one region of a galaxy could conceivably be cancelled out by enhancement in another region, leading to the conclusion that the star formation was unaffected.

Hector will provide the spectral resolution, spatial resolution and sample size required to disentangle how the ages, star formation rates and star formation histories of AGN host galaxies compare to those of inactive star forming galaxies matched in stellar mass and environment, as a function of AGN luminosity and Eddington ratio. AGN host galaxies are expected to make up only ~10% of the emission line galaxy population (Kewley et al. 2006) and therefore the parent sample must be very large before a statistically significant sample of AGN host galaxies can be amassed. Stellar ages and star formation histories can be calculated using both the D4000/Hdelta indices and stellar population synthesis models. The integral field capability of Hector will allow

us to map the stellar ages and star formation histories across galaxies, providing significant insights into the evolutionary sequences of AGN host galaxies and therefore shedding light on the timescales for, and mechanisms driving, the quenching of star formation. The high spectral resolution of Hector will also facilitate spaxel-by-spaxel decomposition of the AGN and HII region emission line spectra. Such decomposition allows the properties of the AGN and the star formation to be calculated independently, providing a means to self-consistently derive the AGN luminosities, Eddington ratios, star formation rates and stellar masses from a single dataset.

2.3.3 Galaxy metallicities

(Based on text by Brent Groves)

The distribution of gas-phase abundances across a galaxy gives us key insight into the formation history of the galaxy through the pollution of the ISM, and into the feeding of galaxies which should lower the metallicity as pristine gas is accreted onto the galaxy, therefore a correlation between the current and past star formation history and the global metallicity is expected (e.g. Mannucci et al., 2010). However, recent resolved work suggests this may be the case (Sanchez et al. 2013; Ho et al. 2015). Key to solving this issue will be resolved metallicity maps, where we can see the accretion of pristine gas onto the outskirts of galaxies through steep radial metallicity gradients in isolated galaxies, but expect flatter gradients as this pristine gas is brought into the inner regions through interactions (Rich et al., 2012). However it appears a universal metallicity gradient may exist across galaxies in contrast with the expected variation across galaxies in recent work based on ~300 galaxies in the CALIFA survey (Sanchez et al., 2014).

Given this apparent disagreement between surveys it is clear that a larger study is needed. Hector will be the perfect way to disentangle the confusion on where radial metallicity gradients are found and their dependence on galaxy properties and environment. The large Hector IFS will provide sufficient spatial resolution to determine both the metallicity and ionization parameter spatial distributions in each galaxy, while the large sample provides sufficient galaxies that the sample can be separated by environment, mass, star formation rate and other galaxy properties to fully understand the average gradients and dispersion for each galaxy property.

The determination of the spatial distribution of the gas-phase metallicity and ionization parameter across galaxies requires a robust determination of the strong optical lines [OII] 3727,3729, Hβ, [OIII] 5007, Hα, [NII] 6584 and [SII] 6717,6731. Out to $z<0.1$ requires a wavelength range $3700 < \lambda[\text{Å}] < 7400$ with no breaks around key lines. It requires sufficient spectral resolution to resolve the [SII] doublet and the [NII] line from Hα. Increasing spectral resolution enables weaker non-star forming ionization mechanisms such as shocks and AGN to be distinguished using both the different velocities and widths of these components (as shown by Ho et al., 2014 and discussed in the shock science case). Resolving the [SII] doublet allows a determination of the electron densities (or upper limits) across the galaxies.

The addition of the strong [SIII] lines at 8831 and 9069 further increases our abilities to determine the ionization parameter of galaxies, and further constrain the electron density to lower values.

To determine the metallicity and ionization radial gradients within galaxies we require several (> 3) independent spatial elements from R=0 to 2 R_e (requiring at least 15" FOV for typical seeing of 2.2"). Beyond 2 R_e, it has been suggested that metallicity gradients flatten (Sanchez et al.,

2014), therefore to detect this break, we require for some of the brighter galaxies a larger FOV to measure out to ~3 R_e.

2.3.4 Kinemetry

2D kinematics of galaxies can be used to effectively classify disturbed galaxies in order to trace galaxy transformations and the build up of mass in galaxies through mergers at various epochs. Kinemetry is an extension of photometry to the higher order moments of the line of sight velocity distribution. It was developed as a means to quantify asymmetries in stellar velocity (and velocity dispersion) maps. These anomalies may be caused by internal disturbances or by external factors, namely interactions (Krajnovic et al. 2006). Kinemetry contains routines to fit the PA and ellipticity of the input kinematic fields to calculate asymmetry coefficients. Morphological methods using the CAS A, Gini coefficient (Gini 1912) or the M_{20} coefficient (Lotz et al. 2004) are primarily sensitive to signatures of ongoing major mergers, such as double cores and large, bright tidal tails, whereas the visual and kinemetric classifications are able to identify perturbations on a range of scales, including twists, warps and small tails. Quantitative morphological methods identify the broad pattern of light distribution in a galaxy. Small features, such as twists, may be overshadowed in the image by bright spiral arms or region of star formation, which are not present in the velocity field.

Kinemetry on large sample of galaxies with Hector will allow a detailed understanding of the connection between the perturbations and star formation across different environments in the nearby universe.

Kinemetry on the SAMI galaxies (Bloom et al., in prep) has found that the measures of perturbations are not dependent on the R_e sampled by the galaxy (unless there was an unusual case of perturbations only in the outmost parts). The spectral resolution requirements are accurate deblending of emission lines (as discussed in 2.3.5), but only the first component fits maps are used.

2.3.5 Scaling relations using gas rotations and dispersions

The Universal dynamical scaling relation discussed above in 2.1.2 uses a unique combination of stellar and gas velocities and dispersions, but the science case will not be repeated here. The same constraints apply to effectively fitting the emission lines as for the other science in this section.

2.3.6 Mapping star formation from Hα for comparison with environment, morphology, radio emission.

There are many science cases that use Hα as a proxy for star formation and all require accurate deblending of the Hα line out to >1 R_e. These include tracing the distribution of star formation with galaxy radius, cluster radius, environment and stellar mass to identify where and how gas is processed in a galaxy to form stars. This is not detailed separately as it strongly overlaps with several detailed cases above.

2.3.7 Misalignments and the origin of gas in galaxies.

The degree of alignment between the stellar and gas kinematics of a galaxy indicates whether the

gas is of external or internal origin. The ATLAS3D survey (Davis et al. 2011) found a significant difference between the (mis)alignment of gas in galaxies in the Virgo cluster and the field. Early SAMI data points to interesting trends in misalignments with local density and with global density with possible evidence of pre-processing of galaxies in groups as entering a cluster (Bryant et al., in prep). However, statistics on the SAMI sample point to the need for 100,000 galaxies in order to have statistically significant galaxy numbers in bins once divided up by morphology, local environment, global environment and stellar mass. Comparison to the predictions of simulations will be essential to understand these results and that will be much more effective with a large sample. The requirements are the same as for the gas and stellar kinematics cases above, as the same fits are used to measure misalignments.

2.3.8 Environmental processing in filaments and the link to HI

(Specific case raised by Kevin Pimbblet , Dane Kleiner, Heath Jones, Baerbel Koribalski)

Filaments are a distinctly different environment to clusters and are the highways for galaxies to be deposited on denser environments. We know that galaxies can (and do) get transformed before entering clusters but where (environment) and how (mechanism) is not very well understood. Filaments are an attractive site for pre-processing, but it is not clear how the filament environments affect preprocessing compared to say groups. The aim is to directly look for outside-in and inside-out truncation in the filaments by comparing HI data to IFU maps of Hα and [OIII].

The alignment of galaxy spins in filaments has been used as a test for dark matter (Aaragon-Calvo et al. 2007), and the alignment of galaxy pairs in filaments is also a current topic (Tempel et al. 2015).

To investigate these questions, we need to know which galaxies reside in filaments and observe them in multiple wavelengths, combining IFU data with HI stacking or resolved HI from ASKAP (WALLABY) and SKA.

Hector will provide a large sample of galaxies in filaments that can be compared to other environments. This case will include a range of galaxy sizes, each of which must be covered by a minimum of 5 spatial elements across, to resolve star formation and ideally separate bulge and disk components. They would be 6dfGRS-type galaxies with typical surface brightness of 20-21 mag/sq arcsec. The brighter galaxies are typically R_e >10 arcsec and would need to be sampled out to ~1 R_e. Aim to target z<0.1 to match to HI. To resolve star formation requires at least S/N>=5 per pixel at Hα λ6563-7548Å. A secondary, less critical aim is to measure [OII] λ3727-4286Å and Hδ λ4009-4611Å as they will be used to place data points on a Poggianti style plane and recover classes such as k+a, a+k, e(a), e(b), e(c) as well as the ubiquitous k class. The number of bundles is more important than spatial elements.

2.3.9 Discussion of modelling of the constraints on emission line fitting

Rebecca Davies used the line deblending code LZIFU on high resolution spectra that had been taken with the Siding Spring Southern Seyfert Spectroscopic Snapshot Survey (S7; Dopita, Shastri, Davies et. al. 2015) with R=7000 (red) and R=3000 (blue). The S7 was used to simulate lower resolution spectra, refit them with LZIFU and test the impact on deblending emission lines. Details can be found in Rebecca Davies talk at the Hector workshop. In summary, it was found that the current SAMI resolution in the blue arm of R~1700 is not sufficient to deblend lines in many cases, and higher resolution is required to remain competitive with MANGA.

A minimum resolution combination of R_{blue}=3000 and R_{red} = 5000 were required to ensure the errors in the Hα and [OIII] emission line fluxes were degraded by no more than 10% compared to those measured in the R=7000 data. Key emission line ratios remained under 0.02 dex for R_{red} =5000 and R_{blue}=3000, however the line ratio errors increased rapidly when either the blue or red resolution was decreased. This is partly driven by the poor ability to fit multiple components in low-resolution spectra, such that more power gets pushed into the broad fitted components as the resolution decreases. The higher scatter in emission line fluxes and hence ratios that results from lower spectral resolution, makes it significantly more difficult to isolate the main source of ionization on the BPT diagram.

A similar simulation was done by Rebecca McElroy, using SPIRAL data with R~5600 (red) and R~2160 (blue) to test how well she could recover signatures of AGN outflows. She found that resolutions below R_{red} ~4500 and R_{blue} ~1500 would have a significant effect on the ability to measure outflows from AGN. The greatest problem introduced by decreased resolution is the complications it adds to model fitting. Even at the resolution of the original data R_{red} = 5600, R_{blue} = 2160, there are still features in the spectra that are barely resolved. In addition, the increased noise and scatter introduced in the diagnostic dispersion versus [NII]/Hα ratio plots becomes very pronounced below R_{red} ~4500 and R_{blue} ~1500 seriously limiting detection of AGN outflows.

Rebecca Davies also simulated the effect of spectral sampling on emission line fits and products starting with 2 pixel spectral sampling, then degrading the sampling down to 1.2 pixels in Figure 7. The results in all plots worsen significantly for 1.2 pixel sampling, but only worsen slowly between 1.6-2.0 pixel sampling. In terms of the derived quantity of AGN fraction, there is little deterioration in the accuracy of detecting the AGN fraction for sampling between 2.4 to 1.6 pixels/FWHM.

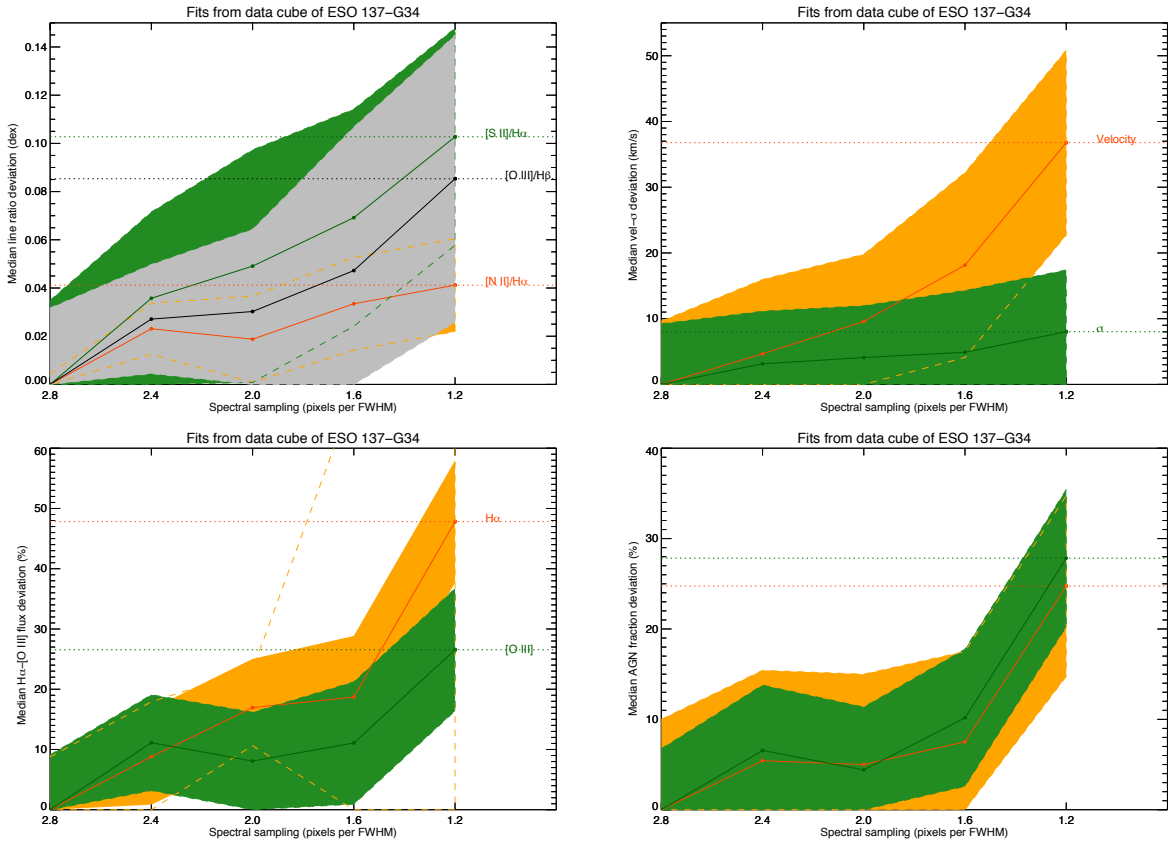

Figure 7: Spectral sampling plotted against line ratios (top left), velocity and velocity dispersion (top right), relative amount of flux in different kinematic components (lower left) and the derived AGN fractions (lower right). From modelling by Rebecca Davies.

The following requirements were identified for deblending emission lines:

- Spectral Resolution: Minimum *requirement*: R=5000 at Hα and R=3000 at [OIII]; *Aim*: R=7000 at both 6500Å and 4500Å (red and blue).
- Wavelength range: *Requirement*: 3700 < λ[Å] < 7500 to get [OII]3727 to [OIII]5007 in the blue and [NII]6548 to [SII]6731 in red out to z~0.1 with a break ideally not near any lines but if essential then NaID λλ5890,5896 is the least important. *Aim*: 3700 < λ[Å] < 7500 with no break around NaID λλ5890,5896.
- Bundle size: *Aim* to get to $2R_e$ in all galaxies and $3R_e$ in some (but maintaining 5 spatial elements minimum). Need highest spatial resolution possible to better resolve SF complexes. At 0.05<z<0.1 Hector will resolve ~1 - 3.6kpc scales (in 1 - 2" seeing), but not individual SF regions which are 10-100pc.
- Flux calibration: Must be better than SAMI.
- Redshift range: *Requirement* is z<0.1.
- Require several (> 5) independent spatial elements from R=0 to $2R_e$ (requiring at least 15" FOV for typical seeing of 2.2"). Plus a larger FOV to measure out to ~$3R_e$ for a subset of brighter galaxies.

2.4 Dark matter

(From Ned Taylor)

Hector has the potential to enable qualitatively new measurements of the dark matter that surrounds galaxies by exploiting the phenomenon of weak gravitational lensing.

The idea underpinning weak lensing as a tool to measuring dark matter halo masses is this: because space is curved in the vicinity of a large mass concentration, galaxies and galaxy clusters act like lenses. As a consequence, the observed images of any background sources viewed in close projection to an intervening galaxy or cluster are both *magnified*, and *distorted*. The degree of distortion depends on the geometry of the source–lens–observer system, and on the mass of the 'lens'. If the 'true' image of the galaxy is known (or can be guessed at), then the degree of distortion can be measured, and the mass of the lens can thus be inferred.

The problem that Hector can solve is knowing or guessing at the 'true' image of any particular galaxy. Hull et al. (2014) have described how the Tully-Fisher relation can be used to derive a prior expectation for the observed inclination, and so apparent axis ratio, of individual disk galaxies. They have argued that such an approach can reduce the effective 'shape noise' in the shear measurement from a single galaxy from $\sigma_\gamma \approx 0.30$ to $\sigma_\gamma < \sim 0.02$. Such an improvement would facilitate qualitatively new kinds of weak lensing studies. In particular, there is the potential that Hector could quantify the scatter in the relation between galaxy stellar and dark matter halo mass, which cannot be directly measured by any existing method.

Observationally, what is needed is only measurements of the maximum projected rotation velocity for each background disk galaxy. This would require only marginal spatial resolution

for the target galaxies, but it would require the detection of Hα out to ~2 times the effective disk scale length. Targets would also need to be at z > ~0.10 (preferably at z > 0.12) in order to have an appreciable chance of being lensed by a foreground galaxy, group, or structure, but z<~0.15 in order to get the velocity fields in a reasonable observing time. However, targets could be preselected — e.g. to be both bright enough in Hα and to have ~1.5" < R_e < ~5" to ensure a useful measurement — since the experiment depends only on the number and redshift distribution of the background galaxies, rather than on any intrinsic properties of the background galaxies themselves.

Requirements for dark matter science case:

- Wavelength range: *Requirement* is Hα at z=0.12 (out to 7400Å allowing for width), and *aim* is to get to 7550Å to get Hα at z=0.15.
- In the absence of useful data at these redder wavelengths, it may be possible to rely on NII and/or the OIII and Hb lines for velocities, but it is more difficult.
- Fibre size and bundle size: good spatial resolution is not critical to get a good measure of Vmax, and large bundles are less important than maximising the multiplexing efficiency of targets.

3 SIMULATIONS TO ASSIST SCIENCE REQUIREMENTS

Before specifically addressing each science requirement in section 4, we first present two simulations that will be used below to set science requirements:

1. **The Hector Survey Simulation** code allows input of a selection function for galaxies then identifies distributions of surface brightness (for comparison to the S/N limits), effective radii, and source densities of galaxies to be observed. This simulation then models the distribution of hexabundle sizes and fibre numbers required to observe the galaxy population to an input number of effective radii (Re, default 2 Re). [Section 3.1]
2. **Hector Total System Simulation** predicts the throughput of Hector and the resulting S/N across the spectrum based on different galaxy types and their spectral shapes. [Section 3.2]

3.1 Hector Survey Simulation: galaxy distributions, surface brightness, effective radii, on-sky densities, IFU and fibre sizes and numbers.

The Hector observations will have constraints set by the seeing and conditions at the site, which limits the surface brightness and the number of spatial elements across a galaxy. Similar limitations have applied to the SAMI galaxy survey selection. A detailed mock simulation has been done, by using GAMA data. While the GAMA catalogue is not an ideal input catalogue for Hector as it is not overhead and therefore requires observations through a higher airmass, it is a good representation of the galaxy distribution in our inevitable selection.

The simulation can take as an input, any cut in the galaxy selection and produce the galaxy distribution in Re, surface brightness and the corresponding hexabundle size distribution to *x* Re. Based on the community consultation *x*=2 has been set as the default value but the simulation can equally take a different input if required. One snapshot of the mock galaxy selection using several realistic galaxy selections is shown in Figure 8. Three different selections are shown:

1. A selection similar to SAMI but fitting to the lower stellar mass limits of the SAMI selection bins up to z<0.1 (blue),
2. An extension of the latter selection to z=0.15 (magenta),
3. A selection (red) aimed to increase the density of objects as much as possible but with minimal effect on the surface brightness distribution. This selection was defined to trace the distribution in surface brightness in the top left panel of Figure 8.

The simulation shows:

- The resultant surface brightness distribution (2nd row, left) is similar for all 3 selections, even though the density of targets is much higher in the red selection. Binning is required for r-band surface brightness >~22.5 mag/arcsec^2.
- The extension to lower stellar mass in the red selection moves the effective radius distribution to lower values (Top row right & 3rd row left). Given that the spatial sampling is limited at 1.5-2arcsec by the seeing, galaxies with R_e < ~2" will have 2 or less spatial elements across the diameter to 1 R_e. On the other hand, such galaxies can be imaged to several Re. A disadvantage of the red selection is that it contains faint surface brightness galaxies with small Re, which will rapidly reach surface brightness limits at >2Re. Binning of the outer regions of those galaxies will be required, and the number of spatial elements across galaxies in the red sample will on average be less than for the blue and magenta samples.
- Ideally we would want to truncate the faint end of the surface brightness distribution. That can only be done by reducing the broad stellar mass coverage because the lower stellar mass galaxies typically form the lowest surface brightness population. However, a broad range in stellar mass is required by many science cases and therefore it is difficult to shift the distribution in stellar mass away from that shown.
- Several science cases have an aim to reach 2R_e in as many galaxies as possible (e.g. stellar kinematics case for angular momentum and most of the emission line cases). Based on the magenta selection, we show the distribution of hexabundle sizes required to image to 2R_e in every galaxy (4th row). Initially an upper limit of ~30" diameter (217 x 100µm fibres, or 469 x 75µm fibres) has been assumed for the maximum bundle size that would be made. This value is adjustable, but was set initially because, as the more outer rings of fibres that are added to the hexagonal pattern, the number of fibres required rapidly increases and hence both the number of hexabundles in the instrument and the survey speed decreases. In addition, this physical hexabundle size is a sensible upper limit for the new fibre processing facility in the SAIL labs (testing may prove it can be pushed to higher diameters). *Given this limit on the hexabundle size, ~87% of galaxies would be imaged to 2R_e using 100µm core hexabundles (or ~89% with 75µm core bundles).*

- If each galaxy is imaged just to $2R_e$, (in the next size bundle up that just fits $2R_e$) then the distribution of hexabundle sizes required is shown in the 4th row (right) and the bottom row compares the number of fibres in total in order to have this distribution and the number of hexabundles that would result across a Hector field of view.
- Given a number of fibres set by the spectrograph design, the completeness to $2R_e$ of the galaxy survey for this distribution of hexabundles can be read from the plots in the lower row (assuming 100 or 75μm core fibres). It is assumed that the minimum hexabundle would have 61 cores and the maximum is 217 cores for 100μm fibre. For example, if the aim is to reach $2R_e$ in 80% of all galaxies using the most hexabundles possible, it will require ~6880 100μm fibres for 100 hexabundles. Alternatively, if say the spectrograph real estate is limited to 8000 fibres maximum, then we can read off the plot that with 100 hexabundles of 100μm cores, ~84% of galaxies would be imaged to 2Re.

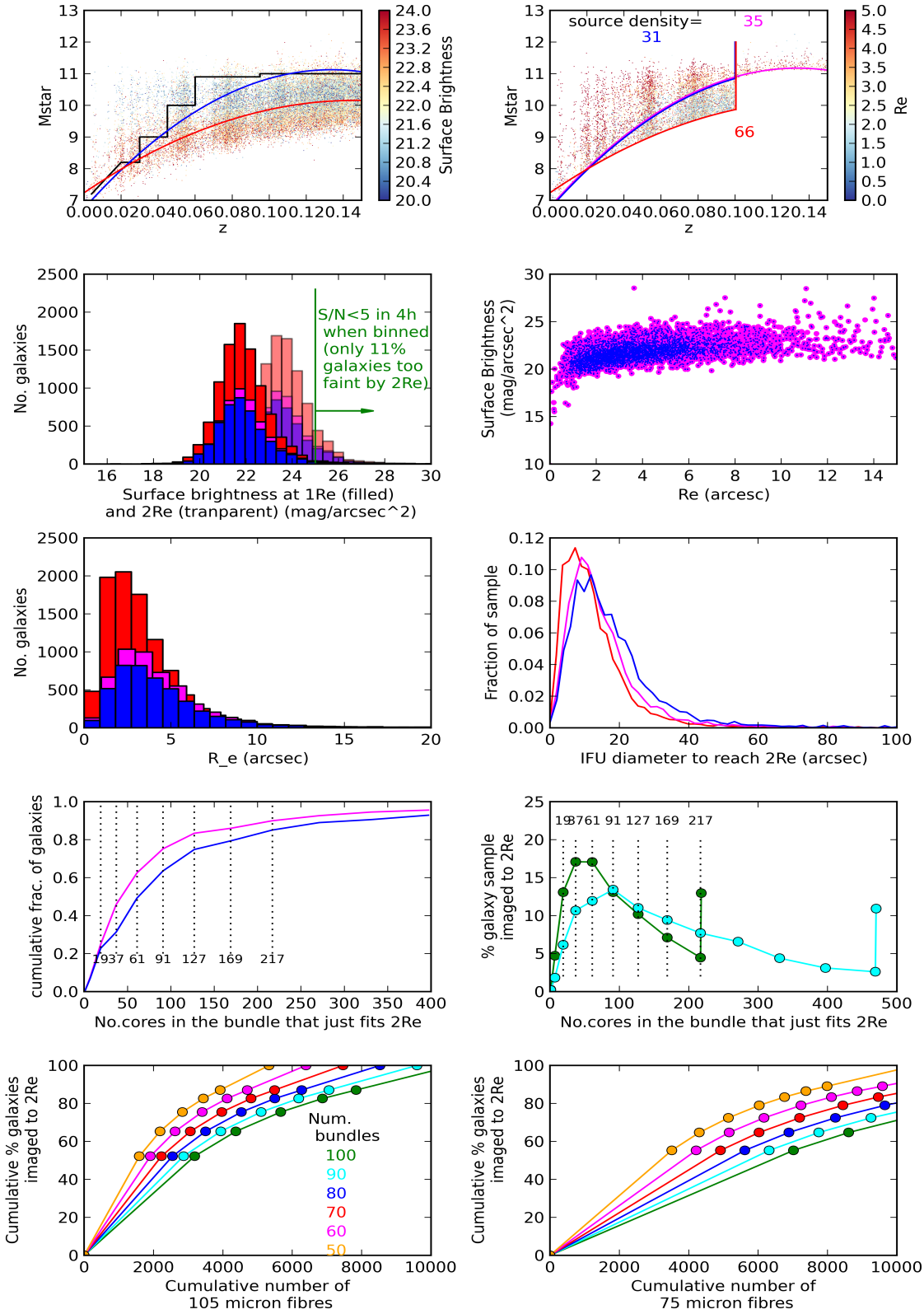

Figure 8: Using the Hector Survey Simulation code, simulations of several possible selections for a Hector galaxy survey based on the GAMA catalogue (with objects flagged as having poor r-band fits removed as the surface brightness and R_e used are in

r-band) are shown. Top row: Redshift and stellar mass plane colour coded by surface brightness at 1R_e in mag/arcsec^2 (left) and effective radius (Re) (right). The black line is the SAMI Galaxy Survey selection, blue is a fit to the lower stellar mass limits of that SAMI selection, red is a more extreme selection that attempts to optimise by surface brightness while still including a broad range in stellar mass. Any other galaxy selections can be simulated with this code, on request. The blue lines and histograms in following panels are based on galaxies above the blue sample cut-off line, including only galaxies with z<0.1, while magenta are galaxies above the same selection cut-off but extended in redshift to z<0.15. The resultant source densities within 1 square degree on sky are given for each of the blue, magenta and red samples defined by galaxies that lie above their respective coloured lines. Second row: Distribution of r-band surface brightness at 1 and 2R_e (left). Note the red selection maintains the same distribution in surface brightness, as the SAMI-style selection in blue. R-band surface brightness at 1R_e vs R_e (right) shows there is little dependence of surface brightness on R_e. Third row: Distribution of R_e for each sample (left). The fraction of the sample vs the diameter required of an IFU to observe each galaxy to 2R_e (right). Fourth row: The number of cores in a hexabundle (and hence angular sizes allowed) is set in increments by the rings of the hexagonal packing. The number of cores for each possible hexabundle size is shown with a dotted line. Galaxies were binned by the next sized core up that fits 2R_e (ie: 4R_e diameter) and the cumulative fraction of the galaxy distribution is shown (left). For example, ~73% and ~81% of galaxies in the blue and magenta samples respectively can be imaged to 2R_e in a hexabundle of 127 cores or less. The % of galaxies from the magenta sample that can be imaged to 2R_e in each bundle size for both 100µm (green) and 75µm (cyan) fibre cores is shown on the right panel. The maximum bundle size likely to be considered for Hector is approximately twice a SAMI bundle or ~30", therefore this plot has been truncated at the closest bundle size to 30" and the final point includes all galaxies larger. Lower Row: Based on the magenta sample; cumulative % of galaxies imaged to 2R_e vs the total number of fibres summed in all the hexabundles where each galaxy is in the next size hexabundle that will image it to 2R_e. Note there is an assumption here that the fraction of galaxies from the previous panel that are not imaged to 2R_e in the largest bundle (~30"), will be in the a bundle of that largest size, and hence are not imaged to 2R_e. The more fibres/bundle, the fewer bundles will be possible given a fixed number of fibres that can be fed to the spectrograph. Therefore this plot sets the number of hexabundles in a Hector field and can be used to check completeness. It is shown for both 100 (left) and 75µm (right) fibres (any size can be simulated on request). E.g. If the limiting number of 100µm fibres in Hector was say ~6,500, then with 90 hexabundles (cyan line), we could image ~82% of all galaxies to 2R_e, but cutting back to 60 hexabundles across the field would allow us to have a range of hexabundle sizes that would image ~100% of the galaxies to 2R_e. The science gains from a larger number of hexabundles imaging most *galaxies to 2R_e outweigh the benefits of imaging* all *galaxies to 2R_e with fewer hexabundles.*

3.2 Hector Total System Simulation: throughput and S/N based on galaxy types

The simulation code has inputs of:

- Selected spectrograph design
- Fibre size (matched to spectrograph design)
- Exposure time, number of dithers, aperture size
- Surface brightness in SDSS AB r-band
- Moon phase (dark or grey)
- Read noise per pixel

Based on modeled throughputs of each component of the Hector system, and extrapolation of sky surface brightness, the throughput and S/N versus wavelength is calculated. Galaxy colours and surface brightness distributions for models defined by Sersic index and stellar mass cuts are calculated and the average values in each galaxy type are used to create the wavelength dependent S/N from the r-band surface brightness.

The simulation predicts a sky to detector throughput shown in Figure 9.

Example output plots from the simulation are shown in Figure 10, assuming 4 hours integration, 7 pointings, 3x4K catadioptric spectrograph design with 1.3Å resolution, 100μm fibres and 1.6" aperture.

This simulation shows:

- Surface brightness of r<21.0 mag/arcsec^2 will have S/N>10 in a single fibre core across most wavelengths for both high and low Sersic index galaxies. This applied to ~20% of galaxies out to 1R_e but only 1% out to 2Re.
- ~60% of galaxies will have r<22.0 mag/arcsec^2 at 1R_e and have sufficient S/N for stellar kinematics fitting even though the S/N <10 in the far blue. Those galaxies will have r~24 mag/ arcsec^2 at 2Re, where the S/N>10 for 24 binned cores.
- Surface brightness of r>~23 require binning of spaxels to achieve S/N>10. Galaxies can be measure with a S/N>5 in 24 binned spectra down to r~25, and therefore only ~1% of the galaxies will not have S/N>5 in the fitted continuum at 1R_e in 24 binned spectra. That is effectively the faint limit in surface brightness.
- While the S/N drops off rapidly in the blue, for stellar kinematic work, where the continuum is fit over a wide wavelength range, the lower S/N in the blue effectively changes the smallest galaxy dispersion measurable (see section 2.1.6 for more details).
- The line most affected by the S/N decline in the blue is [OII]λ3727. If the continuum S/N>5 at 3737Å we expect to be able to measure [OII]λ3727 in galaxies with emission lines. This is the case for galaxies with r<23 for 24 binned fibres or r<21 for single fibres. S/N>5 in the continuum with R~5000 allows equivalent widths of >~2Å to be measured.

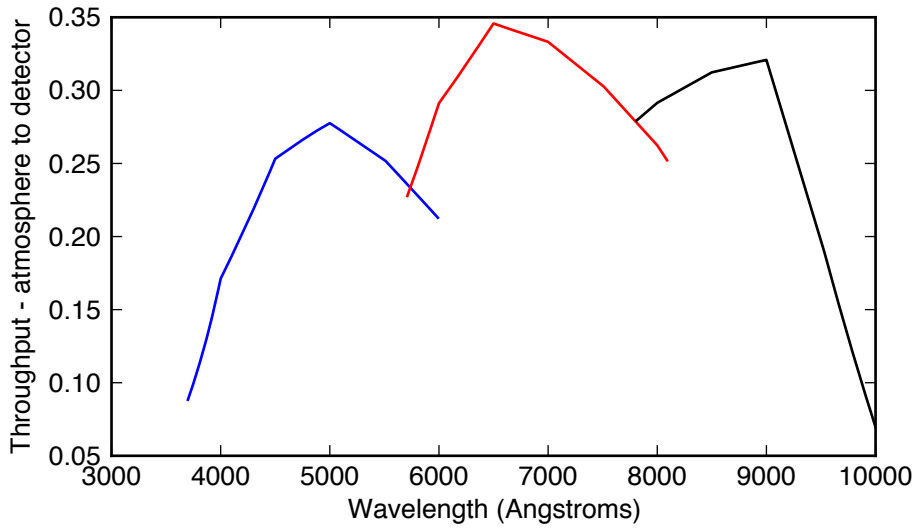

Figure 9: Predicted Hector throughput from sky to detector, based on the Hector Total System Simulation (with the 3x4K catadioptric spectrograph design).

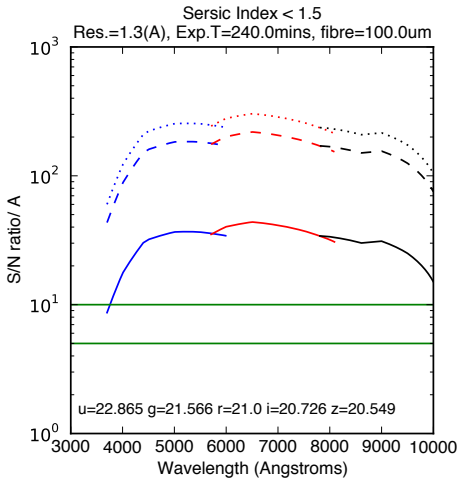

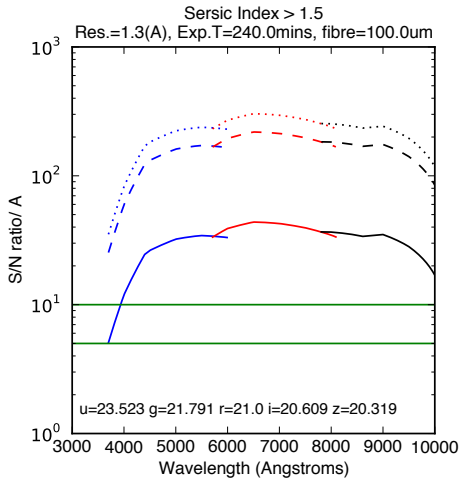

Fraction of galaxies
with r<21.0
at 1 Re: 0.18 0.19 0.2
at 2 Re: 0.01 0.01 0.01

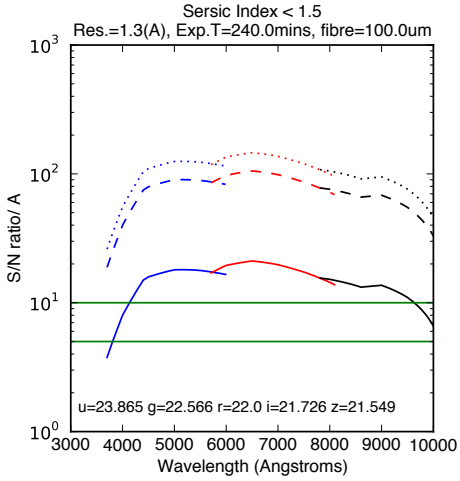

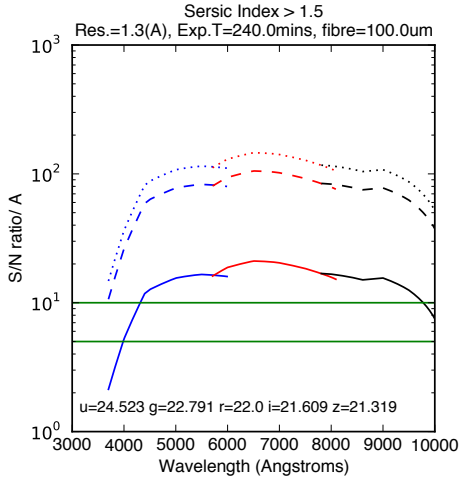

Fraction of galaxies
with r<22.0
at 1 Re: 0.57 0.59 0.6
at 2 Re: 0.06 0.06 0.06

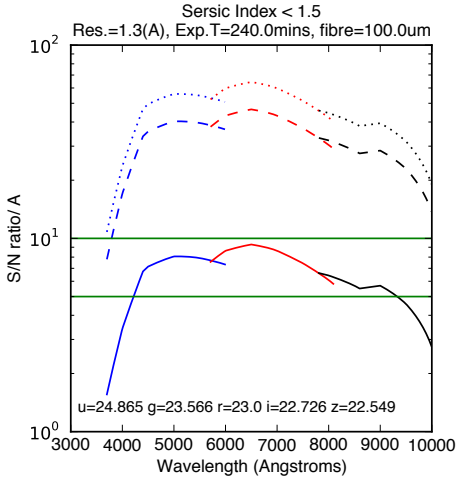

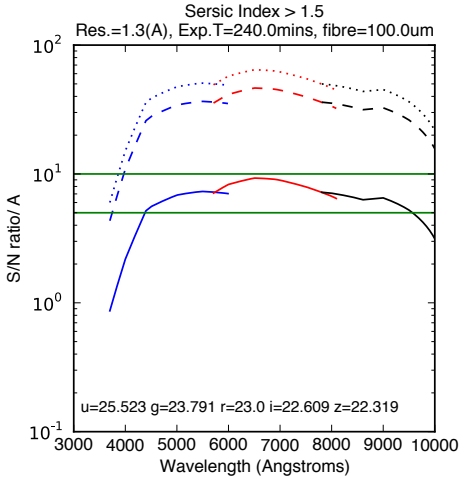

Fraction of galaxies
with r<23.0
at 1 Re: 0.85 0.87 0.86
at 2 Re: 0.28 0.28 0.3

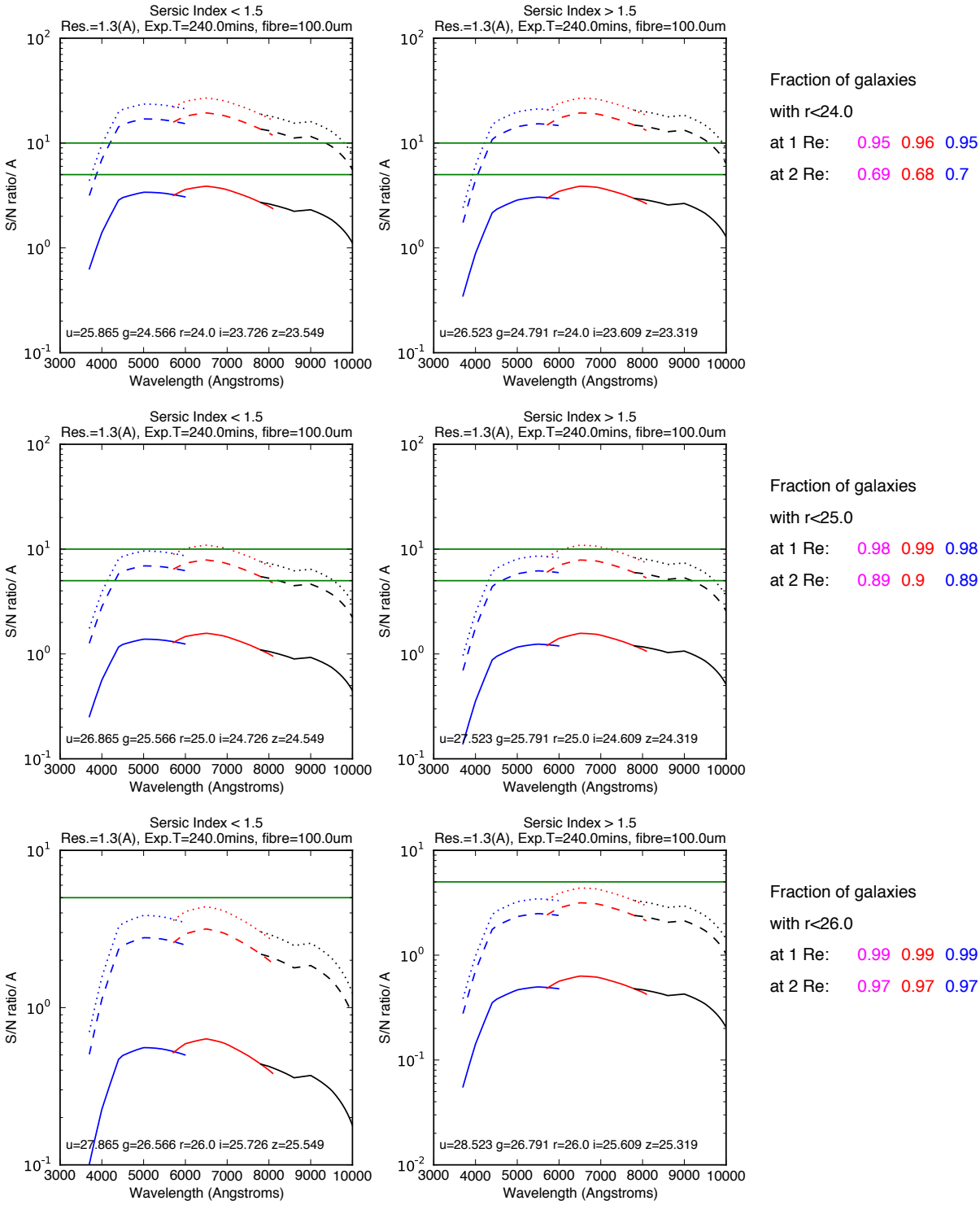

Figure 10: Signal-to-noise in 1.6" aperture (1 core) vs wavelength from the Hector Total System Simulation software for 4 hours integration, 7 pointings, 3x4K catadioptric spectrograph design with 1.3Å resolution, 100µm fibres and 1.6" aperture in dark sky conditions. Galaxies were divided by both a stellar mass cut of 10^{10} M_*/M_{sol} and separately by Sersic index. Only the results for the Sersic index <1.5 (left) and >1.5 (right) are shown here as the Sersic cut forms similar populations to that of the stellar

mass cut. The green lines mark a S/N of 5 and 10/Å. Each row is for galaxy models in which the r (SDSS AB) magnitude of the galaxy at $1R_e$ was r=21.0 to 26.0 (in 1 magnitude steps per row), and the modelled galaxy colours of each population gave the surface brightness across each band as listed within each plot window. Values in magenta, red and blue on the right show the fraction of galaxies in the simulated survey from Figure 8 (matching the same colour) that are brighter than the r-band surface brightness for the corresponding plot at $1R_e$ and at 2Re. The solid lines are S/N in 1 fibre core, and the dashed and dotted are for 24 and 48 cores binned (ie: the outer ring of 61-core and 217-core hexabundles) respectively. S/N plots for any other combination of observing times, spectrograph, resolution and galaxy models are available from the Hector Total System Simulator.

4 SCIENCE REQUIREMENTS

4.1 Wavelength Coverage

Figure 11 and Table 2 list the essential emission and absorption lines and the science cases they satisfy. Note that if there was to be a wavelength break between arms of the spectrographs, the windows allowing a break without impacting key lines are highlighted in Figure 3. The main redshift survey to fulfil the bulk of the key science cases will at a minimum extend to z=0.1 and may potentially extend to z=0.15 (see the Hector Survey Simulation in section 4.4.3). The dark matter science case also has a requirement of z=0.12 and an aim of z=0.15. The requirement is that allowed gaps between lines not be larger than 5889-6280Å for z<0.1, and the aim is for no wavelength gap. These values allow a 20Å window around the lines. These limits are set by Fe3553 at z=0.1 and [OI] at all redshifts. NaID would then be unavailable at z<0.065, however NaID has been highlighted by emission line, stellar population and stellar kinematic science cases as desirable but not as critical as the other lines.

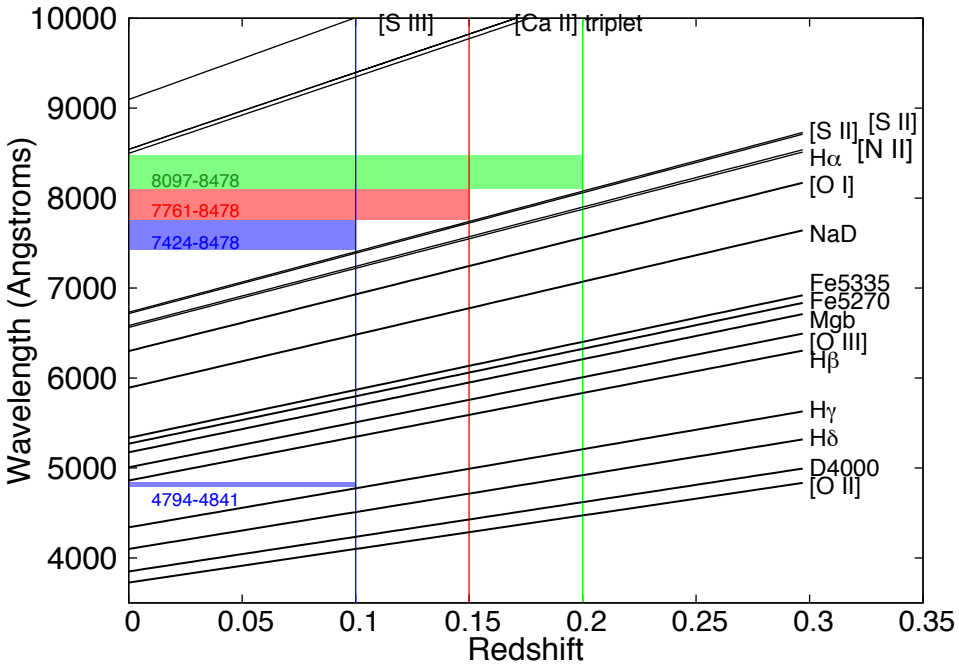

Figure 11: Wavelength coverage vs redshift for key emission and absorption lines. Lines not shown here are generally substantially weaker and are therefore less useful. The coloured stripes with wavelength ranges in Å mark the wavelength regions (allowing a +/-20Åwindow) not *required to be covered in order to observe the lines shown up to redshifts of 0.1 (blue), 0.15 (red) and 0.2 (green).*

Table 2: Wavelength range for key emission lines required for Hector. Need to allow a 20 Å window either side of the listed wavelengths.

Line	λ_{rest}	$\lambda_{z=0.1}$	$\lambda_{z=0.15}$	$\lambda_{z=0.2}$	**Comment**
[OII]	3727	4099.7	4286.05	4472.4	Probe of electron density, star formation measure, tracer of gas kinematics
D4000	3850	4235	4427.5	4620	Age of the underlying stellar population.
Hδ	4100	4510	4715	4920	Useful for stellar populations.
Hγ	4340	4774	4991	5208	Useful for stellar populations.
Hβ	4861	5347.1	5590.15	5833.2	Essential for BPT (tracing gas and ionization properties.
[OIII]	5007	5507	5758	6008	Essential for BPT.

MgB	5174	5691	5950	6209	Stellar kinematics and stellar populations.
Fe5270	5270	5797	6061	6324	Important for stellar populations.
Fe5335	5335	5869	6135	6402	Important for stellar populations.
NaD	5892	6481	6776	7070	Useful for stellar populations, emission line diagnostics and kinematics.
[OI]	6300	6930	7245	7560	Useful diagnostic line.
Hα	6563	7219	7547	7876	Essential for BPT
[NII]	6583	7241	7570	7900	Essential for BPT.
[SII]	6716/6731	7388/7404	7723/7741	8059/8077	Good for measuring densities.
[CaII]	8498-8662	9348-9528	9773-9961	10198-10394	Kinematics and metallicity but complicated by sky brightness.
[SIII]	9096	10006	10460	10915	Kinematics (shocks), metallicity & temperature measure. Good for BPT. Complicated by sky brightness.
Paδ & Paγ	10049 & 10938	11054 & 12032	11556 & 12579	12059 & 13126	Good for measuring reddening, but would need a very red arm.

4.1.1 The case for a 'far' red arm beyond ~8000Å

Arguments in favour of a 'far' red arm (from McDermid's Hector workshop talk):

1. Red region traces old stars, which results in a cleaner bulge/disk decomposition.
2. Includes the Na I λλ8183, 8195Å absorption line doublet and the Wing-Ford molecular FeH spectral absorption band at λ9916Å. These are used to trace stars with masses <0.3 M_{sol} in order to constrain the faint end of the stellar initial mass function (IMF) and stellar mass-to-light ratio.
3. Longer wavelength regions also may help to constrain stellar populations, metallicities and ages.
4. New instruments such as MANGA and MUSE cover these far-red wavelengths and will unlock new discovery space.

Arguments against a 'far' red arm:

1. Cost
2. Much harder to reach the aimed <<1% sky subtraction in the far red where the sky background is high and varies on rapid timescales. However, R>~5000 should be able to resolve out the sky lines.
3. Requires good telluric correction.

4. Needs red-optimised detectors to prevent fringing.

REQ-001 Wavelength Coverage: Hector shall provide wavelength coverage from 372.7-776.1 nm, with a goal for continuous coverage and a requirement of the only gap being the smallest break possible within the range 588.9-628.0 nm. The design shall not preclude a future upgrade path to extend the wavelength coverage to 1000 nm.

4.2 Spectral Resolution and sampling

The tightest constraints on the spectral resolution come from the emission line science cases that require accurate deblending of lines. The minimum requirements for emission line science closely match the requirement for stellar kinematics. Stellar populations are not as restrictive.

Resolution	**Science Case**
Instrumental resolution 1.3Å over 2 pixels across all wavelengths	Stellar kinematics
Requirement of 8.4Å FWHM (σ=280km/s at 3850Å) and target of 2.5Å FWHM (σ=84km/s at 3850Å).	Stellar populations
Minimum requirement: R=5000 at Hα (1.3Å) and R=3000 at [OIII] (1.7Å); Ideal requirement: R=7000 at both 6500Å (0.93Å) and 4500Å(0.64Å).	Most emission line science cases plus Dark matter proposal

4.2.1 Modelling of spectral sampling for stellar kinematics

The van de Sande report models the effect of spectral sampling for different resolutions, on the measurement of σ, h_3 and h_4. Lower sampling at higher spectral resolution gave lower errors on h_3 and h_4 measures for S/N=10, but the effect was less pronounced for higher S/N. The accompanying reference document "Fitting_kinematics_using_SAMI_examples.pdf" shows that low σ values are found in high mass galaxies, not just in low-mass galaxies, and therefore low sigma needs to be measurable across the full stellar mass range.

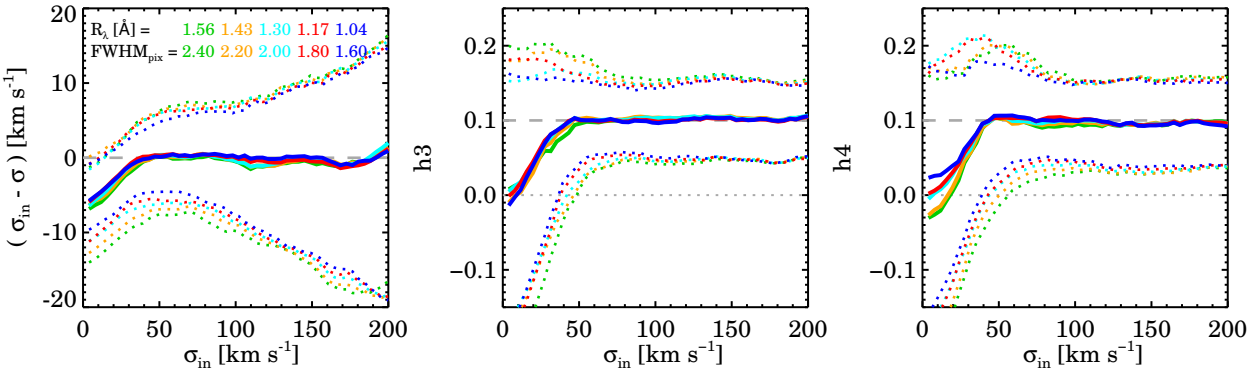

Figure 12: Comparison of the spectral sampling and resolution for the same modelling as presented in Figure 3. A higher resolution with lower sampling (blue) performs slightly better than lower resolution with higher sampling (green) for S/N=10. This effect is less marked at higher S/N.

Summary of key points for resolution:

- Decreasing the resolution to 1.5Å gives only 2% gain in readnoise, only meets emission line requirements just by 5700Å, the continuum minimum σ achievable increases (worsens) by ~10km/s, and it doesn't meet the Hα R>5000 requirement.
- Increasing the resolution to 1Å gives 5% worse readnoise fraction, meets the R>3000 requirement throughout the blue arm and the continuum minimum σ achievable improves (decreases) by ~5km/s.
- 1.3Å spectral resolution is the minimum for the emission line science requirements and higher resolution presents much smaller gains for continuum science. It is the best balance for all science cases.

REQ-002 Spectral Resolution: Hector shall provide an instrumental spectral resolution of at least 0.13 nm from 372.7-776.1 nm with 2+/-0.2 pixel FWHM spectral sampling (requirement). It is desirable (goal) to have an average spectral resolution of at least R=7000 over the range 650-760 nm, and an average spectral resolution of at least R=5000 over the range 776-1000 nm (if this waveband is included).

4.3 S/N requirements

Stellar kinematics requires continuum S/N>10 from 4700-7000Å and ideally 3700-7000Å (see section 2.1.6 for full discussion), stellar populations requires continuum S/N>20/Å in each binned element (see section 2.2), while emission line cases require line S/N>5/Å out to 2Re. S/N

requirements are most constrained by the continuum S/N as emission line S/N is variable among galaxy types and difficult to predict.

The surface brightness decreases with R_e and therefore S/N is closely linked to the galaxy R_e required within a hexabundle. Binning of spaxels can be used to improve S/N in the outskirts of galaxies as long as a minimum number of spatial elements is maintained. The minimum number of spatial elements across a galaxy required by stellar kinematics, stellar populations and most emission line science is 5. Figure 13 left (from Allen et al. 2015, fig.18 right) shows that the SAMI instrument achieves a continuum S/N>10 per binned spaxel for >5 spatial elements across the galaxy in 96% of galaxies overall and 83% of galaxies with mass $<10^{9.5}M_*/M_\odot$. It further shows that the effective number of spatial elements of a given continuum S/N is highly affected by stellar mass which is in turn correlated with surface brightness at 1 or 2 R_e (see Figure 8, top left panel). Therefore the lower stellar mass galaxies will have a lower continuum S/N, which reduces (but not to zero, see section 2.1.6) the fraction of lower stellar mass galaxy observations that will be useful for stellar kinematics and stellar populations. However, many of the lower stellar mass galaxies discussed as unachievable for the stellar kinematics science will be crucial for the emission line science cases as lower mass galaxies typically have higher emission line S/N. Emission line S/N requirements are more difficult to predict, as galaxies vary greatly in emission line strengths, but Figure 13 right (Allen et al. 2015; fig 19 right) has shown that in the lower stellar mass regions, most of the galaxies have emission-line S/N>5 in tens to 100% of the spaxels. Therefore they comfortably have > 10 spatial elements across the galaxy. Some of the higher stellar mass galaxies will not have 3 spatial elements to S/N=5 but nevertheless, the sample that meets the emission line S/N>5 for >3 spatial elements will include the full range in stellar mass based on the improved predicted throughput of Hector over SAMI.

The particular parameters chosen to run in the Hector Total System Simulation code shown in Figure 10, were selected based on the requirements of the stellar kinematics science (particularly the 1.3Å resolution) as that is the science with the most stringent S/N requirement (see detailed discussion in 2.1.6). Therefore the result of that simulation can set realistic estimates of the requirements for Hector. We note that the central surface brightness is ~2 magnitudes brighter than that at $1R_e$ and hence the required S/N is more easily met in a single fibre core. The constraints should instead be set by the S/N in binned cores at 1 and 2Re.

Based on that simulation we can realistically expect to achieve:

- For high stellar mass or Sersic index>1.5 galaxies, S/N>10 over 4700-7000Å (see Table 1 also) in 24 binned cores, for an r(AB SDSS)-band surface brightness of 24.2 mag/arcsec^2 and that surface brightness will be found in ~96% of all galaxies (in the blue/magenta simulated samples, not just high stellar mass galaxies) at $1R_e$ and 75% at $2R_e$ (see also Figure 8 row 2 left). An instrument that meets that requirement will also achieve S/N=50 over 4700-7000Å for r<22.4 mag/arcsec^2 in 24 binned cores in 73% of galaxies. That is sufficient to meet the stellar kinematics science case that favours predominantly galaxies at higher stellar mass (see galaxy dispersion arguments in section 2.1.6 and in the supporting document "Fitting_kinematics_using_SAMI_examples.pdf").
- For low stellar mass or Sersic index<1.5 galaxies, S/N>10 over 4700-7000Å in 24 binned cores should be achieved for r<24.5 mag/arcsec^2, or 98 and 82% of all galaxies (in the blue/magenta simulated samples) at 1 and 2 R_e respectively. Fewer of these will have measureable stellar velocity dispersions, but this S/N limit also favours the

emission line science that dominates among this low Sersic index range

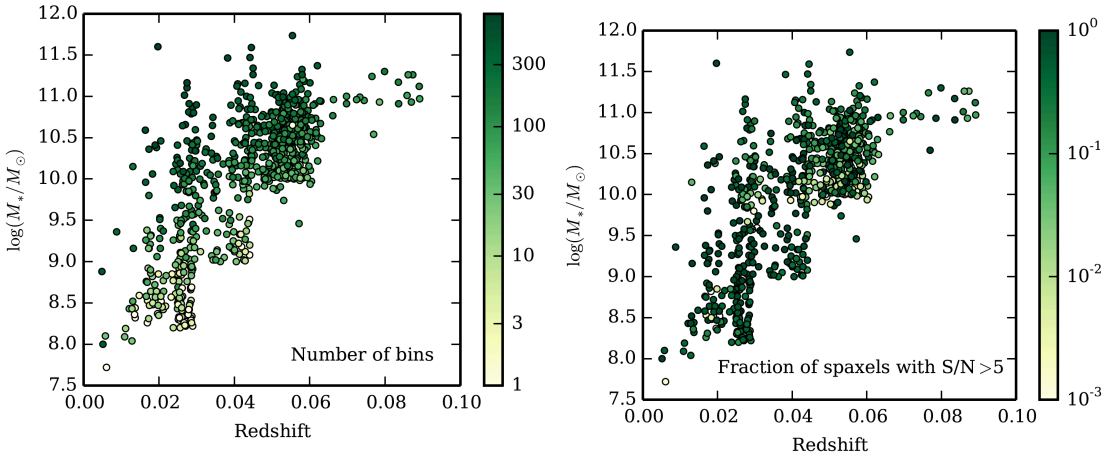

Figure 13: Left: Number of bins formed by adaptive binning with a continuum S/N limit of 10/pix. Right: Fraction of spaxels within the field of view for which H_ is detected with S/N>5.

REQ-003: Hector shall obtain an extended object sensitivity of r(SDSS AB)=24.2mag/arcsec^2 in a 240 minute (requirement), 210 minute (goal) observation with SNR=10/Å from 470.0-700.0 nm and SNR>2/Å at 372.7nm (assuming galaxy colours of g-r=0.79 at 1Re) for 7 dither observations when binned by 24x1.6" cores in dark time (Vsky=21.5, Bsky=22.0 or g=22.0) as well as a 500 minute (requirement), 440 minute (goal) observation during grey time (Vsky=19.0, Bsky=18.5 or g=21.0).

4.3.1 Field configuration times

S/N values discussed above require ~240mins of exposure time per field on average, in order to complete the Hector galaxy survey. Each field requires flat and arc frames to be taken at the start and end and the IFUs moved to the next field. The resulting overheads are 2 x (the alignment of the flat field screen, flat field exposure and readout, arc setup, arc exposure and readout) plus positioning of the IFUs onto each object in the field, and the telescope acquisition of the field. To minimise this combined overhead, the fast positioning of the IFUs and the CCD read times can be optimised. The aim is to complete the arc and flat field within 5 mins each time (start and end of science exposures). If the IFUs can then be positioned within 5 mins, the total overhead for changing fields is 15 mins, or ~6%, which is approximately half of the overheads currently with SAMI. At worst, if the IFU positioning takes 10 minutes per field, the overheads would be 20 mins or ~8%. The faster the repositioning can be done, the better the chance of completing 2 full 4 hour fields in a night, and the more nights that can be achieved as the nights get shorter. Field configuration time is also crucial on weather affected nights when several partial fields may need to be completed and therefore repositioning must occur more times on those nights. Furthermore,

different pointings for a given field can be split up to optimise for airmass if the configuration time is very short.

REQ-004: Field Configuration Time: It shall be possible to slew, reconfigure, acquire, and commence guiding on a new field with Hector in less than 10 minutes (requirement), < 5 mins (aim).

4.4 Hexabundle format and size requirements

4.4.1 Supersampled hexabundles

The original proposal for Hector aimed for a new format of hexabundles in which the centres of the bundles would have fibre cores that are half the size of those on the outskirts. The aim was to achieve finer spatial resolution in the region where most galaxies have higher S/N. Luke Barnes modelled the effect of supersampled hexabundles by using stars and different mock galaxies, then reconstructing the final cube after "observing", dithering, and cubing images by the same method as for SAMI. Barnes' report is an appended document to this report.

The most important conclusion is illustrated in Table 3 that includes data reproduced from Table 2 of Barnes' report. Results are shown for the simulation of a stellar psf with different size fibre cores in the hexabundle. As the star is smaller than the super sampled region, it makes no difference to the reconstructed psf if this is the core size in the centre of a supersampled bundle or if all cores are the same size in the hexabundle. The advantage of supersampled bundles will come from higher resolution and hence a closer reconstruction of the input psf in the final cube. The 5th column gives the ratio of the final to input psf for 3 different seeing conditions (good, median and bad). In median seeing, the psf is increased by 21, 15, and 11% in the 100, 75 and 50µm core hexabundles respectively. Therefore the advantage of supersampling to say 50µm cores in a 100µm core bundle would be a resolution gain of just 10%.

As the seeing variation during an individual exposure and between different pointings in the dither pattern, typically varies by at least 10% and often much more, the gain from the smaller cores will be lost in the seeing variations of the site.

Super sampled hexabundles introduce significantly more complexity both in the hexabundle manufacture, but also in the requirement for two different spectrographs. Given the mediocre gain in resolution, the added complexity suggests supersampling is not justified.

Table 3: Comparison of reconstructed images for hexabundles with different fibre core sizes.

Hexabundle core size (μm)	Dither radius (arcsec)	Drop factor	Input seeing FWHM (arcsec)	Ratio of reconstructed to input point spread function (psf) FWHM.
50	0.33	0.5	1.8	1.11
50	0.33	0.5	1.1	1.23
50	0.33	0.5	2.5	1.06
75	0.50	0.5	1.8	1.15
75	0.50	0.5	1.1	1.30
75	0.50	0.5	2.5	1.08
100	0.67	0.5	1.8	1.21
100	0.67	0.5	1.1	1.35
100	0.67	0.5	2.5	1.13

4.4.2 Fibre cores sizes and read noise

The Hector Total System Simulator code has been used to compare S/N for 100μm and 66μm-core fibres based on the 3x4K transmissive spectrograph design (with an assumption of similar spectrograph throughput to the catadioptric design) for the 66μm fibres and the 3x4K catadioptric design for 100μm fibres. The S/N plots for an r (SDSS AB)=25.0mag galaxy through the 66μm fibres is shown in Figure 14 and can be compared to the equivalent plot for the 100μm cores in the 5th row of Figure 10. It is notable that while the smaller fibres attract a larger read noise in the far blue (read noise fraction of total counts is 0.19 for 66μm cores compared to 0.12 for 100μm cores at 3700Å for these example parameters), the read noise difference has a very small impact on the S/N.

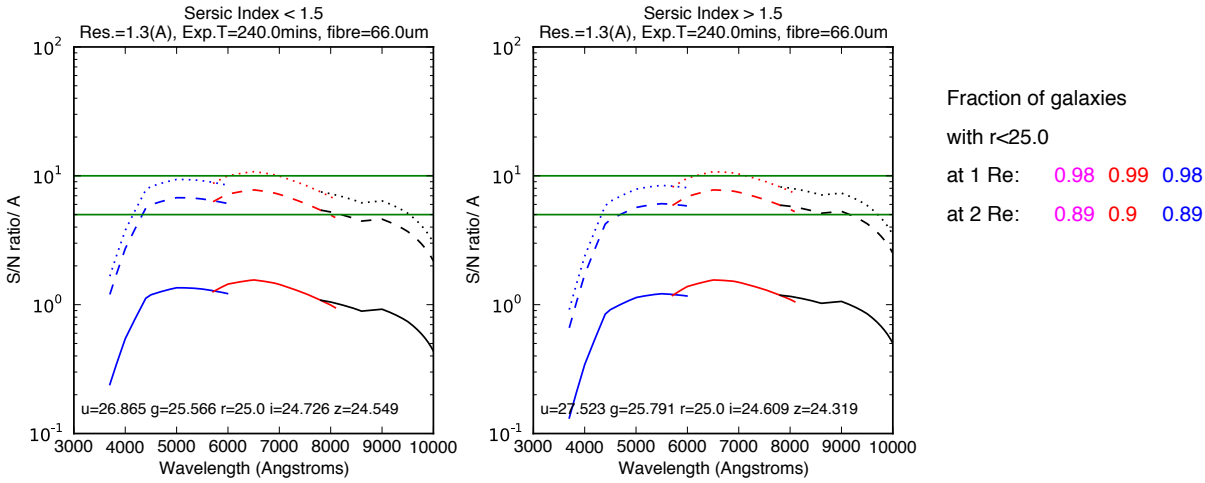

Figure 14: Signal-to-noise in 1.6" aperture vs wavelength for 66µm-core fibre and the 3x4K transmissive spectrograph design, for comparison to the 100µm-core catadioptric option the 3rd row of Figure 10. The galaxy models are for a galaxy with r (SDSS AB) magnitude at 1R_e of r=25.0 assuming 66µm core fibre, 240 minute exposure with 7 dither pointings, 1.3Å spectral resolution over 2 pixels in dark sky conditions.

Based on the Hector Total System Simulator, examples of the read noise contribution to the total counts are shown in Figure 15.

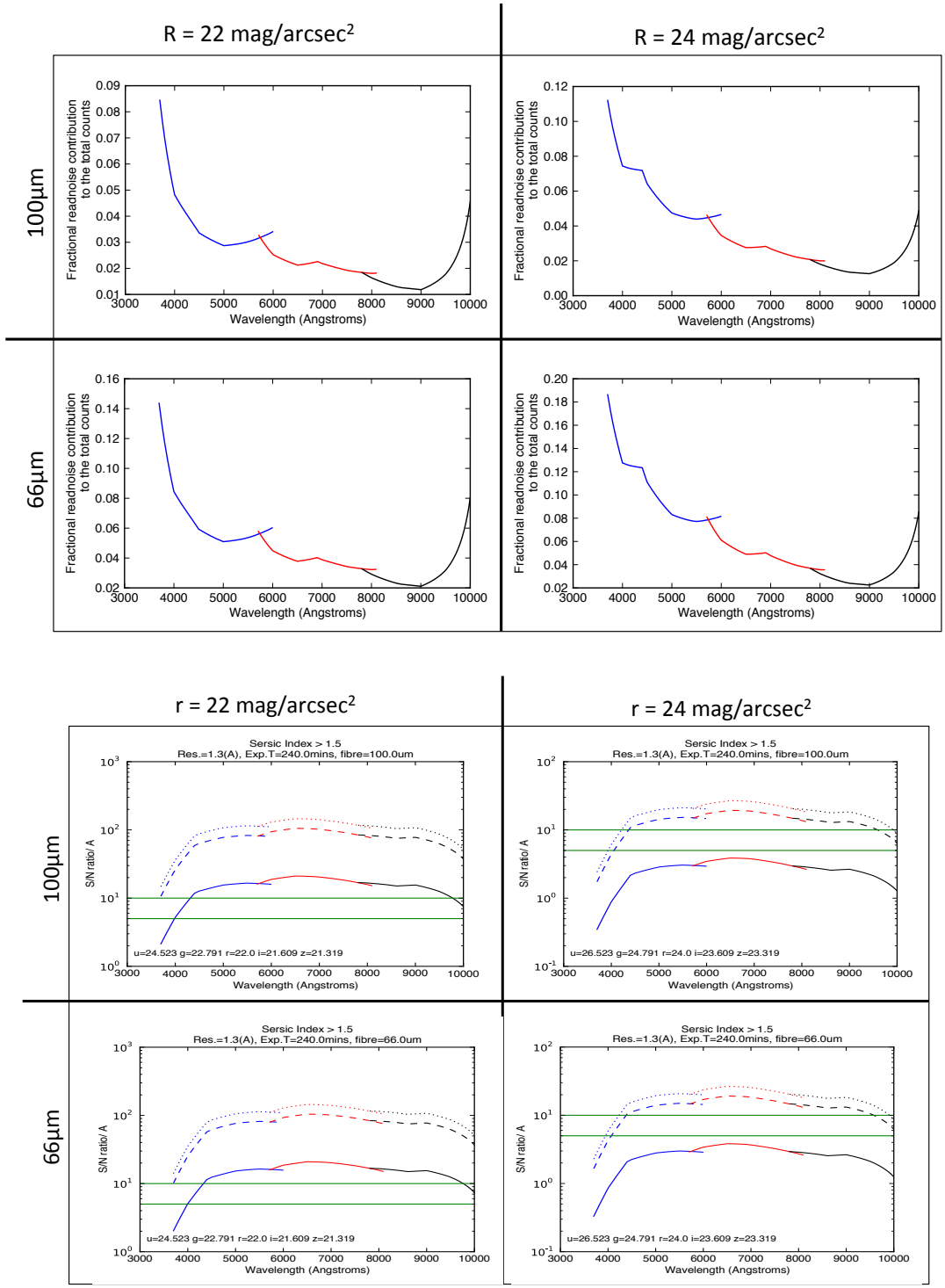

Figure 15: Top group of 4 panels: Fractional contribution of the read noise to the total counts for surface brightness of 22 and 24 mag/arcsec² and for 100µm (1.6") core from the catadiotric spectrograph model and 66µm (1.06") core from the transmissive spectrograph model based on the Hector Total System Simulator. Lower group of 4 panels: The S/N per Å in panels matching the top group.

Direct estimates of the decrease in efficiency due to read noise (read noise fractional hit, or the increased efficiency required to compensate for read noise) for various other spectrograph and fibre size scenarios have been calculated by Will Saunders in Table 4.

Table 4: Effective % throughput penalty due to read noise. η is the efficiency and s is the continuum sky flux (assumed to be 250 photons/s/μm/m^2/arcsec^2 at all wavelengths). In the far blue (~3730Å to 4000Å), the expected efficiency is η~0.08 to 0.15 based on the Hector system throughput simulator for F/1.2 catadioptric design with 1.3Å resolution. These values are approximately twice the throughput currently being achieved with SAMI (Bryant et al. 2015). This gain would necessarily come from the spectrograph and top end having improved throughput because the atmosphere, primary mirror and fibre throughputs will stay the same. The corresponding values for ηs are 20 at ~3730Å and 37 at ~4000Å. Therefore with a resolution of 1.3Å (R=λ/dλ~2869 at ~3730Å) and direct imaging, the read noise hit with 100μm core fibres and F/1.2 camera speed will be ~21%, but rapidly improving by 4000Å to 13%. Values for other potential spectrograph designs are also shown.

Camera speed (fiber size, sampling)		F/1.2 (100μm, 2.2pix)				F/1.65 (75μm, 2.2pix)				F/2.2 (50μm, 2.0pix)		
ηs	Read Noise: Pupil / *Direct*	1 Å	1.3 Å	1.5 Å	2 Å	1 Å	1.3 Å	1.5 Å	2 Å	1 Å	1.5 Å	2 Å
15	2.0 e$^-$		19				31					
	2.2 e$^-$ */2.0 e$^-$*											
	2.2 e$^-$		26				40					
20	2.0 e$^-$	19	15	13	10	30	25	23	18	44	34	28
	2.2 e$^-$ */2.0 e$^-$*	22		16	13	35		27	21	49	39	33
	2.2 e$^-$	26	21	19	15	40	34	31	25	54	44	37
30	2.0 e$^-$	13		9	7	23		16	13	34	26	21
	2.2 e$^-$ */2.0 e$^-$*	16		11	9	27		19	15	39	30	24
	2.2 e$^-$	19		13	10	31		23	18	44	34	28

37	2.0 e^- 2.2 e^- */2.0 e^-* *2.2 e^-*		9 13				15 22					
50	2.0 e^- 2.2 e^- */2.0 e^-* *2.2 e^-*	8 10 12		6 7 9	4 5 7	15 18 21		10 13 15	8 10 12	24 28 32	17 21 24	13 16 19

REQ-005: Spatial Sampling: The on-sky diameter for each IFU spatial element shall be between 1.0-1.8 arcsec (requirement), 1.6+/-0.2 arcsec (goal).

4.4.3 Galaxy sizes, source densities and the impact on bundle sizes

The field-of-view of SAMI means that the core science mostly comes from the analysis of the very inner regions of galaxies (i.e., within one effective radius). Extension of the hexabundles (or IFU) to >>1R_e would allow additional work on merging, environmental impact, and the dynamical, enrichment and star formation histories of galaxies. Competitive instruments such as CALIFA and MANGA partly probe to higher R_e, but will not have the sample size of Hector. Without that spatial coverage, Hector would remain at a disadvantage compared to these smaller surveys. Moreover, the typical atmospheric conditions at Siding Spring, implies that an increased radius is more efficient at increasing the number of independent elements in a bundle rather than supersampling. A field of view twice as big as the current SAMI bundle has several advantages:

1) Increase of the number of independent elements in a bundle,

2) Ability to investigate the very outer parts (i.e., up to two R_e) and/or improve our knowledge of the very inner parts of galaxies,

3) Bridge the current gap between the SAMI field-of-view and the spatial resolution of upcoming ASKAP HI surveys because a 30" diameter bundle would be a better match to the ASKAP resolution. HI would then complete the picture beyond the Hector radius.

4) Remain competitive against other IFU instruments.

The trade-off however is that if every IFU was twice a SAMI hexabundle diameter, then Hector would have many fewer IFUs for the same number of spectrographs. Therefore, the Hector Galaxy Simulation in Section 3.1 models the distribution of R_e in the simulated Hector galaxy

survey, and the impact on bundle size. The lower row shows the number of hexabundles required to image every galaxy in the simulation to 2Re, given a minimum hexabundle size of 61 cores and a maximum of 217 cores (see section 3.1 for details). The distribution of sizes for the IFUs can then be selected from this simulation to meet the science aim of $2R_e$ in each galaxy, once the total fibre numbers are set by the budget and spectrograph design.

REQ-006 IFU size and format: Hector shall provide at least 2 IFU sizes with hexagonally-packed equally-sized fibre cores. The number of hexabundles of each size will be guided by the total number of fibres and the distribution of bundles to reach $2R_e$, as modeled by the Hector Survey Simulation code with an aim to reach $2R_e$ in 90% of galaxies.

4.4.4 Sky fibre distance from hexabundle

In the case that the IFUs are hexabundles and the positioner is a starbug, this section explores the feasibility (based on galaxy profiles) of externally mounting hexabundles in starbugs.

If the hexabundles are mounted in the centre of a starbug, it is likely the footprint of that starbug will need to be increased from that designed for single fibres, in order to have a larger vacuum to offset the additional torque from the weight of many fibres. A larger footprint affects the configuration of fields because close galaxies cannot then be observed if the source density requires only a single pass on each field.

An alternative format is being considered, in which the hexaundle would be mounted (cantilevered) on the outside of the starbug with 2 sky fibres also mounted on the outside equally spaced around the bug as illustrated in Figure 17. This would have several advantages:

1. The starbugs could be rotated to align 2 hexabundles very close together.
2. The vacuum area could be increased without impact on the separation of hexabundles.
3. Having the sky fibres on the same starbug reduces the number of starbugs required and hence the support infrastructure is minimised.

In order for this scenario to be feasible, the sky fibres must be far enough away from the galaxy light to be only detecting sky with no galaxy contamination. When the outer radii of 61-core bundles are binned, galaxy continuum can be detected to ~4-5 magnitudes fainter than sky (see Sections 4.6.1 and 3.2). In order to test the distance required to avoid galaxy contamination, the Sersic parameter, surface brightness at $1R_e$ and R_e values from the GAMA catalogue were used to plot the radius of galaxies in the SAMI selection when the surface brightness drops to 2, 3, 4 and 5 magnitudes/arcsec^2 below the sky surface brightness. This was all done in the r-band using a sky brightness for Siding Spring of 21.1 mag/arcsec^2. Figure 16 shows this distribution, along with lines marking the distance of the sky fibre from the galaxy (assumed to be centred in the hexabundles) when the hexabundle is in the centre of a starbug and the sky fibre mounted on the outside (green line) or when the hexabundles and sky fibres are equally spaced around the

outside of the starbug. The magenta line is a minimum distance because it is based on the following conservative assumptions:

1. the radius of the bug is 4.5mm (as in TAIPAN bugs), which is a minimum because a Hector starbug will likely be larger due to additional vacuum area,
2. the sky fibre on the outside is mounted in a ferule that is 1mm diameter (it could be much more for practical purposes),
3. the hexabundle on the outside of the starbug is mounted in a ferule with a diameter of 4mm (given that the fused bundles will have diameters of up to 2mm, the ferule would not be smaller than 4mm).

The orange line in Figure 16 (for the format shown in Figure 17(b)) may be closer to a maximum distance (David Brown, priv comm.) because there may be temperature constraints in having a larger vacuum area in the starbug, and the cantilevers need to retain rigidity.

This analysis shows that a 3-point external mounting of hexabundles and sky fibres will put the sky fibres sufficiently far from the galaxy as to measure the sky with a contribution from the galaxy continuum that is 4 magnitudes fainter than the sky background for >99.9% of galaxies in this selection.

Emission line contribution is variable between galaxies and more difficult to quantify. Christlein & Zaritsky (2008, ApJ 680, 1053) attempted to quantify the maximum radius for detection of Hα emission and they detected Hα up to 1.5 x R25 on average and up to 2 x R25 in some disk galaxies, where R25 is the radius at which the surface brightness in B-band drops to 25 mag/arcsec^2. Similarly, Ferguson et al. 1998 (ApJ, 506 L19) found H-alpha emission out to 2 x R25 in deep narrowband imaging of nearby spiral galaxies. While Figure 16 is in the r-band, the B-band sky brightness at Siding Spring in dark time is 22.5mag/arcsec^2, and therefore the line emission was detected to ~27 mag/arcsec^2 in B which is ~4.5 mag/arcsec^2 fainter than sky, which is between the cyan and black histograms in that figure. However, patches of star formation could potentially occur in the outer disks for a small fraction of disk galaxies, leading to emission line regions at very high radii.

In the small fraction of galaxies that may contaminate sky fibres, the sky fibres on that starbug could not be added in to the total sky frame for that field observation. This can be managed with a priori assessment of potential contamination by a cut in effective radius and surface brightness, and/or eliminating sky spectra with line emission at the galaxy wavelength.

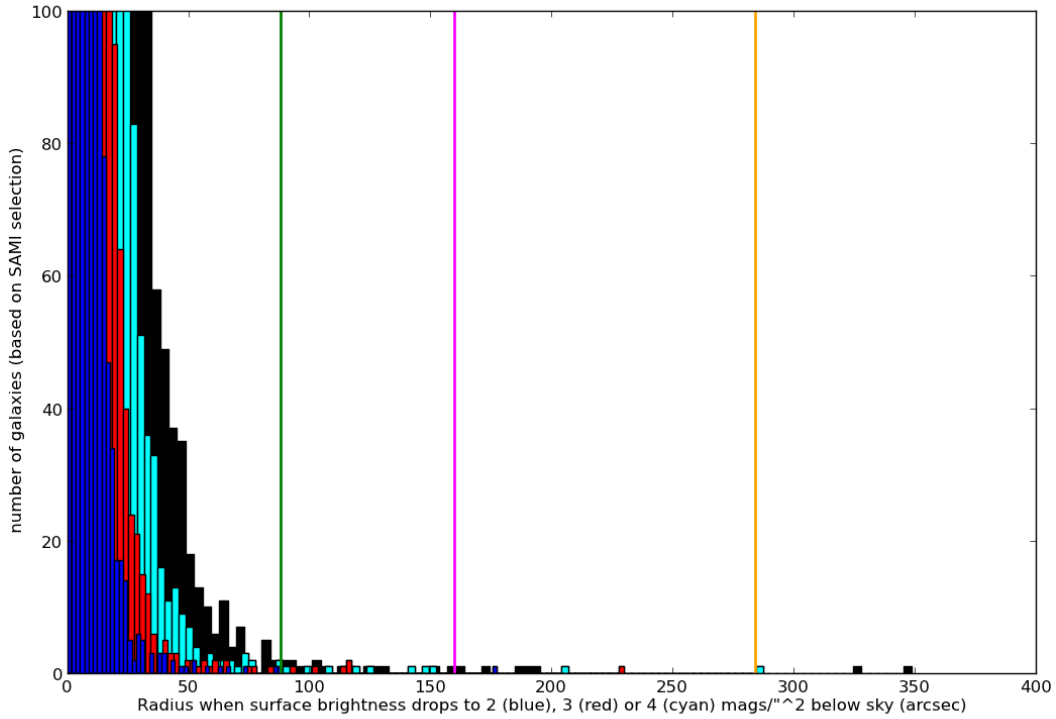

Figure 16: Distribution of the galaxy radius at which the surface brightness drops to 2 (blue), 3 (red), 4 (cyan) and 5 (black) magnitudes/arcsec^2 fainter than the r-band sky brightness at Siding Spring (21.19 mag/arcsec^2 calculated from Johnson/Cousins filter values). The galaxy population included is based on the SAMI-type galaxy selection. The vertical lines mark the minimum radius at which a sky fibre would sit from the galaxy centre if the sky fibre was mounted on the outside of the starbug with the hexabundle centred in the bug (green), or if the hexabundles and 2 sky fibres were mounted equally-spaced around the outside of the starbug (magenta; as in Figure 16(a) and orange as in Figure 16(b)). Therefore as the sky fibre will be positioned where the galaxy is 4 magnitudes fainter (cyan) than the sky brightness for >99.9% of galaxies for both the magenta line and orange lines representing configurations in Figure 17 (a) and (b) respectively, and down to 5 magnitudes/arcsec^2 fainter (black) for >99.87% of galaxies for the orange line configuration. This proposed design for hexabundles and sky fibres to be mounted externally on starbugs is therefore worth investigating.

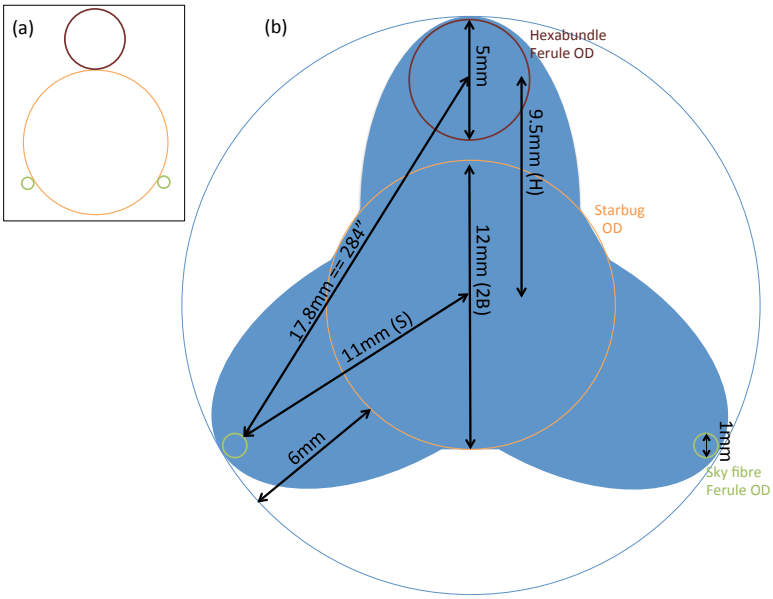

Figure 17: (a) Representations of the potential configurations of hexabundles and sky fibres mounted externally to the star bug. This possibility for starbugs has not yet been tested and is evaluated here only to test the feasibility of this option based on the distance of the sky fibre and the extent of galaxy profiles. The most compact scenario shown in (a) gives the smallest distance that the sky fibre would be mounted from the galaxy. Another realistic scenario representing the larger limits of this distance is shown in (b). In this scenario, the blue shaded region represents some form of rigid support that can take any shape to support the cantilevered sky fibres in their ferule (green circles) and hexabundle in it's ferule (red circle). The balance on this support allows the sky fibres to be mounted at a higher radius from the starbug (orange circle) as they are lighter and smaller than the hexabundle. The starbug has twice the vacuum footprint of the TAIPAN starbugs, which increases the holding power to support the larger torque from the multiple fibres. While all dimensions in this diagram need to be evaluated and tested, a scenario which spaces the sky fibres much further from the hexabundle becomes difficult for mechanical reasons (David Brown; Priv. communication). David noted that previous studies have shown there are temperature issues with a much larger footprint due to the larger vacuum power. Based on this layout, the sky fibre would be 284 arcsec from the galaxy centre, which is beyond the radius at which >99.9% of the galaxies in the SAMI sample have a surface brightness 4 magnitudes/arcsec^2 less than the sky (see Figure 16).

4.4.5 Hexabundle-to-hexabundle distance (exclusion radius)

The exclusion radius or closest distance between two hexabundles, can affect the efficiency of a galaxy survey if it limits the possible tiling configurations. If the hexabundles were mounted in the centre of starbugs 12mm in diameter (Figure 17, but internally mounted) and a 2mm gap is allowed between starbugs then the exclusion distance would be 213 arcsec (14mm). If hexabundles were mounted as described in Figure 17(b), and starbugs were rotated to allow hexabundles to be positioned adjacent to each other with a 2mm gap, then the exclusion distance would be 106 arcsec (7mm). The impact of these two options on tiling was simulated using the GAMA 15h field and a galaxy selection similar to the blue selection in Figure 8, with a source density of 21 objects/sq. degree. The number of tiles required to reach 95% completeness

increased by only 4% when the exclusion distance doubled and the efficiency of those tiles changes from 83% to 86%. Much larger exclusion distances however have a significant impact on the efficiency and tile numbers (for example 600 arcsec exclusion gives a 55% increase in the required tile numbers and overall efficiency of 52%).

4.4.6 Source catalogues

Hector will need parent catalogues from which to select the 100,000 galaxies. The main requirements for the source catalogue are:

- Requires complete galaxy coverage down to beyond our limiting magnitude (integrated r~19.5 mag).
- Requires a source density of >15/sq. degree, which naturally comes from the Hector sources selection based on a complete galaxy catalogue with R~19.5 based on simulations with the GAMA catalogue with stellar mass and redshift limits to give achievable S/N (see section 4.4.3). This source density therefore requires 6700 sq. degrees of sky coverage to reach 100,000 galaxies.
- Desirable to have overlapping data from surveys in other wavebands. In particular HI is essential for gas masses and extended kinematics, and IR to far-IR is beneficial for accurate dust measures. To have synergy with HI before SKA Phase 1, requires targets with z<~0.1.
- Desirable for the survey to go to several magnitudes deeper than our selection in order to have good environmental measures (halo masses, environment densities) for Hector galaxies.
- Broad coverage in RA to ensure that the dark time can be used every month. To achieve this, we would need to move to more equatorial fields in the 9-16h regions, and observe overhead regions around 21-4h
- Sources ideally should be overhead, not equatorial so that the average observed airmass is lower, resulting in lower effective seeing hence better spatial resolution, and observability.

Table 5: Parameters of MOS and imaging surveys that may be complementary or parent surveys for Hector.

	Mag limit	Sky area (deg^2) / sampling	No. galaxies	RA range (deg)	DEC range (deg)	Ancillary data
MOS surveys:						
TAIPAN	r<18	All southern sky	500,000	All	Southern sky	LSST
4MOST/WAVES WIDE	r<22	750	10^6	~ -30≤α≤60	~-30	EUCLID LSST KiDS-S

DESI on Mayall	r<19.5	14,000	$10x10^6$ to z~0.4.		Northern sky	
SDSS3 - BOSS	r<17.8	10,000	$1.5x10^6$	most RAs	North of ~0 deg.	
ASKAP (HI)		All southern sky		-180≤α≤180	<+30	
Imaging surveys:						
DES on Blanco	g,r,i,z,Y <~24	5,000	$200x10^6$ by ~ end 2018	-60≤α≤105 -30≤α≤60 -3≤α≤45 -43≤α≤-3	-65≤δ≤-40 -40≤δ≤-25 -25≤δ≤3 -1≤δ≤1	LSST, DESspec
LSST	u,g,r,i,z,y with r~28 AB mags	All southern sky	20 billion	-180≤α≤180	<+10	
VST/KiDS	u<24.8, g<25.4, r<25.2, i<24.2	N=780; S=720 / ~0.2"/pix ~0.7-1.1" seeing		KiDS-N 174≤α≤240 KiDS-S -30≤α≤52.5	KiDS-N ~0 KiDS-S -26 to -36	WAVES
VISTA/ VIKING	Z, Y, J, H, K	1500				
EUCLID -WIDE	550-900nm<24.5,Y<24, J<24, H<24	15000 / ~0.2"	$1.5x10^9$ from 2020-2026	Nearly all-sky except galactic plane and solar system		
DECam Legacy Survey (selection imaging for DESI	g<24.7, r<23.9, z<23.0	9,500			-18° < δ < +84°	
J-PAS narrow band survey	56 narro-band filters	8,000	14×10^6 from ~2016-2021			

Two clear options for parent catalogues for Hector are the Wide Area VISTA Extra-galactic Survey (WAVES; http://www.wave-survey.org) and the TAIPAN survey.

WAVES-WIDE has the advantage of excellent environment measures as it reaches R=22 mag. WAVES also has substantial ancillary data (WISE [mid-IR], HERSCHEL [far-IR], SKA Ph 1 [HI continuum], eROSITA [X-ray], 4MOST [redshifts], VISTA/VIKING [Near-IR], EUCLID [near-IR], VST/KiDS [optical imaging], GALEX [UV]). However WAVES-WIDE covers 750 sq. degrees of sky only and a single block near RA=0h. WAVES observations will be underway by ~2021 which means we may have to preselect on the photometry as WAVES is observing then obtain the spectroscopy afterwards, but that will not allow redshift pre-selection. Their selection is apparent magnitude-limited and will peak around L*.

TAIPAN has the advantage of coverage of a much larger sky area to 20,000 sq. degrees, but to a shallower depth of r=18, and without as much ancillary data. The RA coverage includes the entire southern sky with 500,000 galaxies or 25 per sq. degree. A likely selection could therefore be a combination of TAIPAN and WAVES (see Figure 18, but since the Hector survey will need to use dark time every month, the bulk of the survey would be with TAIPAN and hence be limited to bright targets with less extensive auxiliary information.

Alternatively a photometric redshift selection from Skymapper main survey data may be possible, but less reliable than spectral redshifts. Other options will need to be investigated.

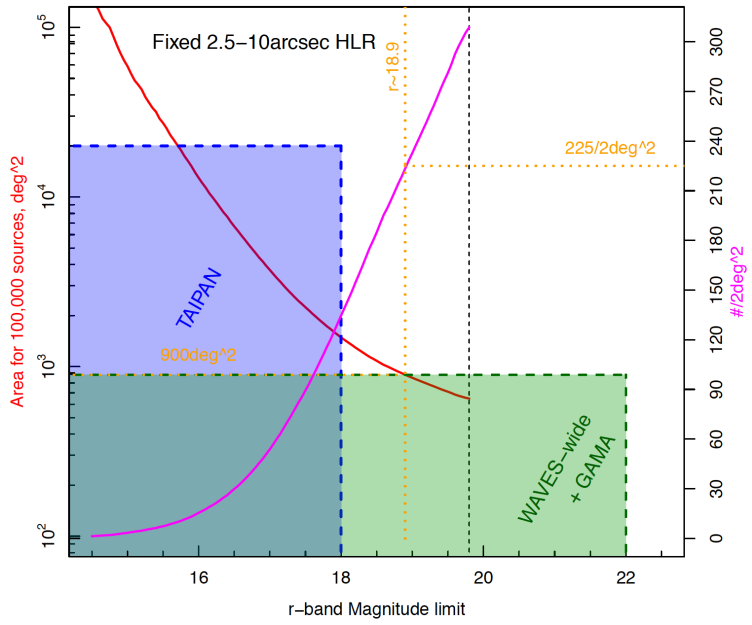

Figure 18: From Hector science workshop talk by Luke Davies: r-band magnitude limit vs area required for 100,000 sources (red, left axes) and vs number of galaxies per 2 sq. degrees (magenta, right axes) for galaxies selected to have 2.5< Re< 10.

4.5 Field of view

Hector aims to complete a survey of ~100,000 galaxies. In order to do so in a competitive time frame, the field of view needs to be large enough (given the source density on sky) to have sufficient IFUs to reach the required multiplex. Table 6 presents scenarios for 1, 2 and 3 degree diameter fields. Three different IFU densities are shown, based on

1. The current density of IFUs in SAMI (15/sq. deg),
2. A realistic increase that can be easily met with slight adjustment to the source selection (20/sq.deg.), and
3. The maximum IFU density (25/sq.deg.) that would still be less than the blue selection (in Figure 8) source density of 31 galaxies/sq.degree.

The Hector galaxy survey competition:

- MANGA – 10,000 galaxies by 2020. If MANGA is extended over the life of Hector, it may amass an additional ~10,000 galaxies per 5 years.
- WEAVE on WHT – has a galaxy evolution survey component that will begin in 2018 and have up to 10,000 galaxies by 2023.

In order for Hector to be revolutionary with a 5-10-fold increase in multiplex over other surveys, the Hector survey therefore needs to be complete within an aim of ~ 5 years. A 5 year survey with 20,000 galaxies per year will double the previous surveys within the first year alone. The sooner the full instrument is on sky, the greater the science gain compared to the competition.

Table 6 shows that a 1-degree field alone is insufficient to be competitive. However in a staged approach, a single Hector spectrograph and 8 new larger hexabundles could be added to the existing 1dF SAMI, resulting in a survey with 25 galaxies/sq. degree. This step would directly contribute to the final Hector instrument as long as the spectrograph was then directly used in Hector and the hexabundles built to be removable from magnetic plugs, to be remounted in starbugs later. The next stage would be the full 3dF instrument. With this approach the AAO will continue to provide useful IFU galaxy observations simultaneously with testing and demonstrating the new spectrographs and hexabundles, plus allowing the software development that will be required in preparation for Hector.

A 2-degree field option is not recommended, as it offers none of the strategic advantages for the AAO going forward that can be realized with a 3df. While potentially offering larger galaxy numbers for a year or so **if** it could be completed 2 years faster than the 3df option, the timeframes are uncertain for both at time of writing and the ongoing productivity if 3df substantially outweighs short term gains in galaxy numbers.

A 3-degree field is required in order to complete a groundbreaking 100,000 galaxy survey and after the initial top end investment, spectrographs and hexabundles can be added in a staged approach if funding is limited. 141 hexabundles would allow 20 galaxies per sq. degree and complete a 100,000 galaxy survey in <5 years. A reduced cost version with ~106 hexabundles in a 3 degree field will complete as many galaxies in 6 years, which remains highly competitive.

The total fibre area (not hexabundle area) covered depends on the fibre size because the incremental angular size of each hexabundle changes. Therefore the listed requirement for total number of IFUs cannot be in terms of angular size. However, as an example, 50 and 100 IFUs of 105μm cores gives a total fibre area of 8530 (4242 fibres) and 17059 (8485 fibres) arcsec^2

respectively, and 50 and 100 IFUs of 75µm cores gives a total fibre area of 9281 (8206 fibres) and 18561 (16412 fibres) arcsec^2 respectively. The requirement in REQ-007 therefore sets a total fibre area of 8530 arcsec^2 and an aim for 17059 arcsec^2 if the fibre cores are 105µm diameter. Equivalent values for any fibre size are available from the Hector Survey Simulation code.

Table 6: Comparison of different fields of view and IFU densities. The number of IFUs is selected to meet the IFU densities of 15, 20 and 25/sq. degree (realistic within the blue galaxy selection). The number of fibres required for each scenario is given based on all IFUs having 61-cores and on an average of 106 fibres per IFU. The latter is based on the galaxy simulation in Figure 8, for 1.6 arcsec fibres, with hexabundles ranging from 61-217 fibres and each sampling galaxies in the blue simulation out to 2Re, giving the average number of fibres per hexabundle as 106. The number of years assumes 10 dark nights per month for 10 months/year (100 nights/yr) and 1.5 fields/night (including weather) when starbugs are used for the 2df and 3df options. Current SAMI is the first row, which assumes no larger than 61-core existing bundles and the current SAMI efficiency of 1 field/night which less efficient than starbugs due to plug plates. Second and third rows assume all hexabundles in the 1df are upgraded to varying sized new bundles. The number of galaxies by the given years assumes the current SAMI galaxy survey is completed in mid-2018 and those 3400 galaxies are not included in these totals, then the SAMI instrument moves to a new survey that takes all dark nights for 10 months per year. An upgrade to new bundles and spectrographs in rows 2-3 is expected to begin observing at the end of 2018. A 2dF option is expected to be observing by the start of 2020 and a 3dF option by the start of 2022. Red numbers assume an upgrade path from a 1df option to the 2 or 3df. The number of fibres required and number of spectrographs becomes unrealistic by the final row.

Field of view (diameter, deg)	**Number of IFUs on galaxies**	**IFU density per sq. degree**	**No. of fibres if 61 fibres/IFU excl. IFUs for secondary standards**	**No. of fibres if average of 106 fibres/IFU excl. IFUs for secondary standards**	**No. of years to complete 100000 galaxy survey**	**No. of galaxies per survey year.**	**No. galaxies by start 2020**	**No. galaxies by start 2022**	**No. galaxies by start 2025**	**No. galaxies by start 2027**	**~No. spectrographs**	**Positioner Plug-plate/starbug**
1	12	15	732	732	56	1200	1800	4200	7800	10200	AAOmega	P
1	16	20	976	1696	42	1600	3200	6400	11200	14400	AAOmega + 1	P

1	20	25	1220	2120	33	2000	4000	8000	14000	18000	AAOmega + 1	P
2	47	15	2867	4982	14	7050						S
2	63	20	3843	6678	11	9450	0 4000	18900 22900	47250 51250	66150 70150	6	S
2	79	25	4819	8374	8.4	11850	0 4000	23700 27700	59250 63250	82950 86950	7	S
3	106	15	6466	11236	6.3	15900	0 4000	0 8000	47700 55700	79500 87500	9	S
3	141	20	8601	14946	4.7	21150	0 4000	0 8000	63450 71450	105750 113750	12	S
3	177	25	10797	18762	3.8	132750					16	S

REQ-007: Multiplex: The Hector instrument shall have: at least 50 IFUs (requirement), at least 100 IFUs (goal).

REQ-008: Field of view: The available field of view shall be at least 3 degrees diameter (requirement). A 2 degree field of view will only be considered as a descope.

4.6 Requirements to meet sky subtraction and flux calibration accuracy.

Based on text from Scott Croom

4.6.1 Sky subtraction

The most critical constraints on sky are due to stellar population analysis and to a lesser degree stellar kinematics. Given the default wavelength coverage of HECTOR, emission line sky subtraction is expected to be a secondary issue. This would not be the case if the HECTOR spectrographs were extended to the far red (e.g. CaT region). A detailed assessment of what is possible requires careful consideration of the current and possible future modes of calibration

and data reduction. This will not be discussed here in detail, but some general comments will be made.

Continuum sky subtraction requirements

Continuum sky subtraction is influenced by flat fielding, spectral extraction (including psf, tramline modeling etc.) and absolute throughout calibration. The requirements on sky subtraction are best defined in the blue continuum where the majority of diagnostic spectral features are found. A second consideration is the degree to which we will bin the data. Greater binning can substantially increase the S/N, particularly in the outer regions of the galaxies (where surface brightness is low and there are many spaxels to co-add). However, this places *much* tighter constraints on sky subtraction precision if we are not to be dominated by systematics. Therefore in Table 7, we will consider two limits for sky subtraction, that for a single fibre aperture (assumed to be 100μm sized with 1.6"), and that for the binning of 24 fibres (the outer ring in a 61-core hexabundle). The outer ring binning gives an increase in S/N of a factor of 5, assuming no systematics. The table below uses the Hector S/N calculator to estimate the S/N (dark sky, 4 hour total exposure with 7 dithers) in a single fibre and in 24 binned fibres at a variety of surface brightnesses. S/N values are an average for the two Sersic model groups (see Section 2 for details). The key point to note here is that we are able to get useful S/N and therefore to useful science down to r~25. Note that the dark night sky is r(SDSS AB)~21.2 mag arcsec^{-2}.

Table 7: Sky subtraction precision requirements for faint surface brightness limits with single and binned fibres.

r-band surface brightness (SDSS AB mag/sq arcsec)	Factor fainter than r=21.2 sky	Single fibre S/N per Å at 5000Å (4 hours)	Binned (24 fibre) S/N per Å at 5000Å (4 hours)	Sky subtraction precision required for 1% spectrophotometry
23.2	6.3	6	31	0.16%
23.7	10.0	3.8	19	0.10%
24.2	15.8	2.5	12	0.063%
24.7	25.1	1.6	8	0.040%

Currently in SAMI the continuum sky residuals are on average at the ~1% level. However, their contributions vary profoundly as a function of wavelength and position on the slit. The wavelength averaged sky subtraction is typically ~2-4% at the edge of the slit, but in the far blue (~4000A), this can be as bad as ~20%. In fitting stellar populations to the Hector data we should be aiming to achieve the best fits that current stellar population models will allow. The MILES (Sanchez-Blazquez et al. 2006) templates which form the current standard have relative spectrophotometric precision of 0.013 mag (rms, internal), which would suggest that we need to limit the impact of flux calibration and sky subtraction to approximately 1% of the object flux. While there are continuum spectral features across the entire spectrum, those in the blue (3700-5200A rest wavelength) are particularly critical, so it is particularly important that an appropriate level of sky contamination is required. The table above shows that for a limiting surface

brightness of r=23.2 mag/sq arcsec, we can obtain S/N~6 in a 4 hour exposure (dark sky, *unbinned*) with Hector. This is close to the faintest limit that we can reliably fit stellar continuum to measure stellar kinematics. To limit the impact of sky subtraction to be less than 1% of the object flux at this limit requires sky subtraction residuals to be less than 0.16%, which is substantially better than is currently achieved with AAOmega (with SAMI or any other fibre front end). When binning the limit is pushed further, so that the requirement at r=24.7 mag/sq arcsec is 0.04%. Note that although the "per A" S/N is low in these cases (S/N~6-8), the broad continuum shape is fitted over the entire spectrum so is sensitive to sky subtraction at a much greater level than the simply per Å S/N would imply. This calculation assumes that the spectral shape of the targets will be similar to the sky, which is not the case in detail.

The estimated limits for sky subtraction should therefore be:

- 0.16% requirement.
- 0.04% goal.
- The above requirements should be met at each wavelength, not just on average.

A further test required to confirm these conclusions more broadly is:

- Simulated low surface brightness observations to directly measure the impact of sky subtraction on stellar population ages, metallicities and kinematics.

REQ-009: Sky subtraction: Hector shall allow sky subtraction to within 0.16% (requirement) with a goal of 0.04% across the full spectrum.

4.6.2 Skyline subtraction requirements

The night sky emission lines in specific spectral regions have a significant impact on the quality of data, particularly in the far red. Given the availability of current PCA techniques and the strength of the night sky lines, our aim should be for sky subtraction for emission lines to be Poisson limited.

4.6.3 Telluric absorption correction

Atmospheric absorption in the red also impacts spectrophotometry (including some of the redder emission lines depending on galaxy redshifts). The requirement here should be to correct for atmospheric absorption bands to a level consistent with the requirements on sky subtraction above. This leads to a requirement for telluric correction at the ~1% level.

4.6.4 Flux calibration

Given the constraints listed above, concerning the quality of spectroscopic stellar templates, the requirement for flux calibration should be 1%.

REQ-010: Flux calibration: Hector shall allow absolute flux calibration of all sources to within 1% across the full spectrum.

4.6.5 Wavelength calibration

I-Ting Ho has used SAMI data to investigate the error on fitting all emission lines over the SAMI wavelength range. SAMI currently achieves 0.05 - 0.1Å wavelength calibration. Figure 19 shows that in >50% of the spaxels that have an Hα S/N>5, the formal fit error produced by the LZIFU simultaneous emission-line fitting software (Ho et al. 2014) is smaller than 0.05Å (~3 km/s). Therefore the formal fit value is underestimating the real error, which is dominated by wavelength calibration at that point. SAMI can't reach better than 0.05 - 0.1Å (3-5 km/s) now.

Wavelength calibration with < 0.05Å velocity error would therefore reduce the actual fit error on the lines however, the gains of going much lower are limited by sampling and how well the psf shape is known. The absolute calibration of 0.05Å in SAMI is ~10% channel width in the blue and has not been shown to limit any science case. The aim for Hector therefore should to do somewhat better but a requirement of 0.05Å will be adequate in most cases, and there is not a strong science driver to achieve substantially better wavelength calibration accuracy.

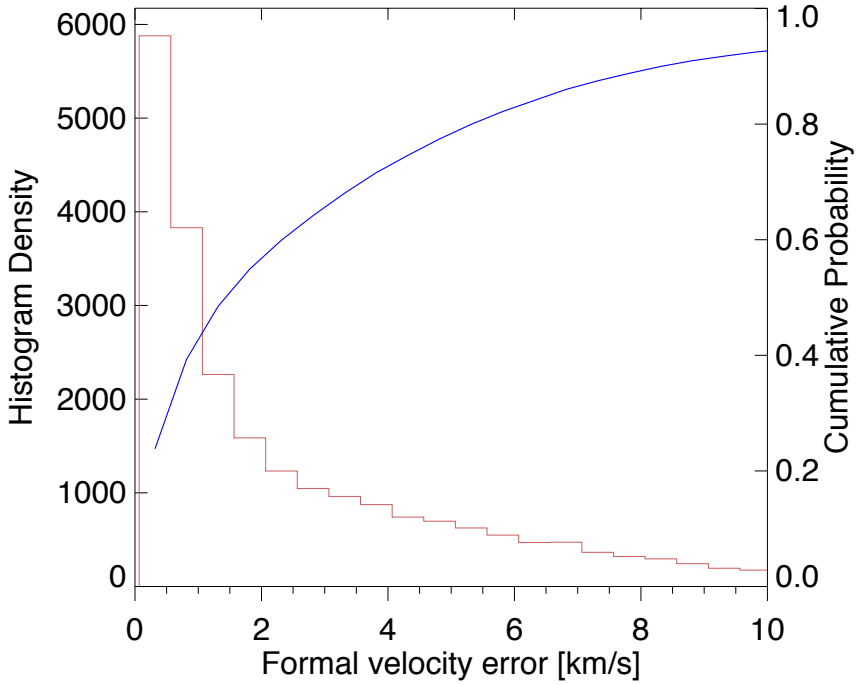

Figure 19: In LZIFU emission-line fitting software (Ho et al. 2014), the lines are all tied to the same velocity, but the blue and red wavelengths are allowed to have a small shift. This shift is a fitting parameter (formal velocity error), and is allowed to vary +/- 1 blue channel width (+/-1.04A). This Figure aims to test how many pixels have smaller formal velocity errors than 0.05 - 0.1A (~ 3 - 5km/s). The formal velocity error is plotted for the top 50 galaxies after an Hα S/N>5 cut was applied. A significant fraction (>50%) of good (Hα line) pixels has nominal velocity errors < 3 km/s. Therefore, in SAMI, when

S/N of Hα is good, we are often limited by wavelength calibration error, and the best velocity accuracy we can achieve now is ~3-5 km/s.

REQ-011: Wavelength calibration: It shall be possible to obtain an absolute wavelength calibration of all spectra to within: 0.005 nm (requirement), 0.0025 nm (goal).

4.6.6 Cross talk

Overlap of the spatial profiles between adjacent fibres on the detector affects how easily those profiles can be separated to give the correct flux. The fitting of the profiles strongly depends on the profile shape, and that will change from fibre-to-fibre both across a bundle and between bundles and at different positions on sky. The flux error from fitting the overlapping fibres, must be small enough that in combination with scattered light, errors in the cubing process from imperfect atmospheric dispersion correction, sky subtraction and flat fielding errors, the total flux calibration remains <1%.

Calibration accuracy is the *most important criteria* that will give Hector a substantial advantage above SAMI or MANGA. Hector's improved spectral resolution advantage will be lost if the calibration is not substantially better than SAMI, as that is a current hindrance to SAMI science. Therefore, fewer fibres/IFUs that are well calibrated due to a larger spacing on the detector is significantly more favorable to the science than more fibres/IFUs with poorer or uncertain quality data.

4.7 Competing and complementary surveys

Table 8 lists other surveys that may be competing with or complementary to Hector. By 2020 complementary higher redshift surveys will already be in place, including ~5000 emission line objects at z~1-2 from KMOS on the VLT, and likely several thousand z<3 galaxies from VIRUS on HET. EUCLIDS imaging/spectroscopic survey at z>0.7 and WFIRST at z>1 will progressively follow after 2020. These are a resource for evolutionary science cases.

Table 8: Other surveys that may be competing or complimentary to Hector.

Instrument	On Sky date	Resolution B/R (R=dλ/	Wavelength range (Å)	Galaxy survey size	Selection criteria	Radial coverage (R_e or arcsec diameter)	Typical seeing (")	Input spaxel size (")

		λ)						
SAMI	2012	1730/ 4500	3700-5700 6300-7400	3400	0.004<z<0.1 10^7<M<10^{12}	12x15" (1-2 R_e)	1.8	1.6
MANGA	2014	2000	3600- 10300	10,000	M>10^9	1.5-2.5	0.9"	2.0
CALIFA	2010	1650/850	3700-7500	600	45"<D_{25}<80"	1x2"-2.5"	0.9"	2.7
WEAVE on WHT (galaxy evolution componenet of survey)	2018	10,000	3800- 10,000	10,000	HI (APERTIF) selected.	20x11"x12"	0.7"	1.3"
MEGARA on GTC 10m	2017	5000/ 10,000	~3600-9700	Only 2 IFUs		1x12.5"x11.3" / 1x8.5"x6.7"	0.67"	0.62/0.42
MUSE; PMAS; WiFeS	All current.	2000/4000;	4650-9300; ~3600-9000; 3300-9200	Single object at a time, but ~few thousand by 2020.		60 x 60"; 74 x 65"; 38 x 25"	0.5-2"	0.2"; 2.7"; 0.5"
MOS IFU on GMT	>2021				Could do survey to z~0.5.	Maximum 20 arcmin telescope FoV.		

5 SCIENCE CASES LINKED TO INSTRUMENT PARAMETERS

*Table 9: Science cases linked to science requirements. If the science **requirement** specified for Hector meets the **aims** of a science case it is coloured green, if it only meets the **requirements** of a science case it is orange and if it does not meet a science case aims or requirements it is red.*

Science Requirement: / **Science Case:**	REQ-001 Wavelength coverage	REQ-002 Spectral Res.	REQ-003 Sensitivity.	REQ-004 Field config time	REQ-005 IFU spatial elements	REQ-006 IFU size & format	REQ-007 Multiplex	REQ-008 Field of view	REQ-009 Sky subtraction	REQ-010 Flux calibration	REQ-011 Wavelength calibration
Stellar kinematics											
Stellar populations											
Emission-line science											

6 SUMMARY OF SCIENCE REQUIREMENTS

REQ-001 Wavelength Coverage: Hector shall provide wavelength coverage from 372.7-776.1 nm, with a goal for continuous coverage and a requirement of the only gap being the smallest break possible within the range 588.9-628.0 nm. The design shall not preclude a future upgrade path to extend the wavelength coverage to 1000 nm.

REQ-002 Spectral Resolution: Hector shall provide an instrumental spectral resolution of at least 0.13 nm from 372.7-776.1 nm with 2+/-0.2 pixel FWHM spectral sampling (requirement). It is desirable (goal) to have an average spectral resolution of at least R=7000 over the range 650-760 nm, and an average spectral resolution of at least R=5000 over the range 776-1000 nm (if this waveband is included).

REQ-003: Sensitivity: Hector shall obtain an extended object sensitivity of r(SDSS AB)=24.2mag/arcsec^2 in a 240 minute (requirement), 210 minute (goal) observation with SNR=10/Å from 470.0-700.0 nm and SNR>2/Å at 372.7nm (assuming galaxy colours of g-r=0.79 at 1Re) for 7 dither observations when binned by 24x1.6" cores in dark time (Vsky=21.5, Bsky=22.0 or g=22.0) as well as a 500 minute (requirement), 440 minute (goal) observation during grey time (Vsky=19.0, Bsky=18.5 or g=21.0).

REQ-004: Field Configuration Time: It shall be possible to slew, reconfigure, acquire, and commence guiding on a new field with Hector in less than 10 minutes (requirement), < 5 mins (aim).

REQ-005: Spatial Sampling: The on-sky diameter for each IFU spatial element shall be between 1.0-1.8 arcsec (requirement), 1.6+/-0.2 arcsec (goal).

REQ-006 IFU size and format: Hector shall provide at least 2 IFU sizes with hexagonally-packed equally-sized fibre cores. The number of hexabundles of each size will be guided by the total number of fibres and the distribution of bundles to reach $2R_e$, as modeled by the Hector Survey Simulation code with an aim to reach $2R_e$ in 90% of galaxies.

REQ-007: Multiplex: The Hector instrument shall have: at least 50 IFUs (requirement), at least 100 IFUs (goal).

REQ-008: Field of view: The available field of view shall be at least 3 degrees diameter (requirement). A 2 degree field of view will only be considered as a descope.

REQ-009: Sky subtraction: Hector shall allow sky subtraction to within 0.16% (requirement) with a goal of 0.04% across the full spectrum.

REQ-010: Flux calibration: Hector shall allow absolute flux calibration of all sources to within 1% across the full spectrum.

REQ-011: Wavelength calibration: It shall be possible to obtain an absolute wavelength calibration of all spectra to within: 0.005 nm (requirement), 0.0025 nm (goal).

REFERENCES

Aragón-Calvo M.A., Jones B.J.T., van de Weygaert R., van der Hulst J.M., 2007 A&A, 474, 315

Benson & Bower 2011, MNRAS 410, 2653

Bernardi M., Nichol R.C., Sheth R.K., Miller C.J., Brinkmann J., 2006, AJ, 131, 1288

Blanton & Moustakas, 2009, ARA&A, 47, 159

Cappellari et al. 2011 MNRAS, 416, 1680

Cooper M.C., Tremonti C.A., Newman J.A., Zabludoff A.I., 2008, MNRAS, 390, 245

Dubois Y., et al., 2014, MNRAS, 444, 1453

Efremov Y., 2011, ARep, 55, 108

Emsellem et al. 2011 MNRAS, 414, 888

Fogarty L., et al., 2014, MNRAS, 443, 485

Forero-Romero J. E., Hoffman Y., Gottlo ̈ber S., Klypin A., Yepes G., 2009, MNRAS, 396, 1815

Gomez P.L., et al. 2003, Ap. J, 584, 210

Hahn O., Porciani C., Carollo C. M., Dekel A., 2007, MNRAS, 375, 489

Hahn O., et al., 2007, MNRAS, 381**,** 41

Ho I.- T. et al., 2014, MNRAS, 444, 3894

Ho I.- T. et al., 2015, in press.

Hoffman Y., Metuki O., Yepes G., Gottlo ̈ber S., Forero-Romero J.E., Libeskind N.I., Knebe A., 2012 MNRAS 425, 2049

Kauffmann G., et al., 2004, MNRAS, 353, 713

Kitaura F., Angulo R.E., Hoffman Y., Gottlöber S., 2012 MNRAS, 425, 2422

Knebe A., et al. 2011 MNRAS, 415, 2293

Krajnovi´c et al. 2011 MNRAS, 414, 2923

Leroy A.K., et al. 2008, AJ, 136, 2782

Lewis I., et al. 2002, MNRAS, 334, 673

Libeskind N.I., Hoffman Y., Forero-Romero J., Gottlöber S., Knebe A., Steinmetz M., Klypin A., 2013 MNRAS, 428, 2489

Muldrew et al., 2012, MNRAS, 2670, 82

Naab T., et al., 2014, MNRAS, 444, 3357

Park C., Choi Y.Y., Vogeley M.S., Gott J.R.I., Blanton M.R., 2007, ApJ, 658, 898

Peng Y., et al., 2010, ApJ, 721, 193

Peng Y., Lilly S.J., Renzini A., Carollo M., 2012, ApJ, 757, 4

Robotham A., et al., 2013, MNRAS, 431, 167

Romanowsky A.J. & Fall S.M., 2012, ApJS, 203, 17

Rownd B.K., Young J.S., 1999, AJ, 118, 670

Sanchez-Blazquez P., et al., 2006, MNRAS, 371, 703

Slosar A., White M., 2009, JCAP, 6, 9

Sousbie T., Pichon C., Colombi S., Novikov D., Pogosyan D., 2008 MNRAS, 383, 1655

Sousbie, T., 2011 MNRAS 414, 350

Sousbie, T., Pichon C., Kawahara H., 2011, MNRAS, 414, 384

Tempel, E., & Libeskind, N. I. 2013, ApJ, 775, L42

Tempel, E., Stoica, R. S., & Saar, E. 2013, MNRAS, 428, 1827

Tremonti C.A., et al., 2004, ApJ, 613, 898

Trowland H., Lewis G. & Bland-Hawthorn J., 2013, ApJ 762, 72

Varela J., Betancort-Rijo J., Trujillo I., Ricciardelli E., 2012, ApJ, 744, 82

Zhang, Y., Yang, X., Wang, H., et al. 2015, ApJ, 798, 17

DRAFT REVISION HISTORY

Revision	Date	Author	Comments
0.1	June 2015	JJB	Not even first proper draft yet – needs much work!!!
0.2	August 2015	JJB	Additional Science case added, plus more detail on read noise and S/N in the blue.
0.3-0.5	Sept 2015	JJB	Additions to requirements.
0.6	Oct 2015	JJB	Editing of science case by Scott Croom, plus additions to requirements by JJB.
0.7	Oct 2015	JJB	Minor additions following Science Review meeting. Largest change is to Table 6 and section 4.5.
1.0	Nov 2015	JJB	Wording format of the requirements adjusted to meet instrument team requests.